

# Configuration Control in the Synthesis of Homo- and Heteroleptic Bis(oxazolinyphenolato/thiazolinyphenolato) Chelate Ligand Complexes of Oxorhenium(V): Isomer Effect on Ancillary Ligand Exchange Dynamics and Implications for Perchlorate Reduction Catalysis

Jinyong Liu,<sup>\*,†,§</sup> Dimao Wu,<sup>||</sup> Xiaoge Su,<sup>⊥</sup> Mengwei Han,<sup>†</sup> Susana Y. Kimura,<sup>†</sup> Danielle L. Gray,<sup>‡</sup> John R. Shapley,<sup>‡</sup> Mahdi M. Abu-Omar,<sup>#</sup> Charles J. Werth,<sup>∇</sup> and Timothy J. Strathmann<sup>\*,§</sup>

<sup>†</sup>Department of Civil and Environmental Engineering and <sup>‡</sup>Department of Chemistry, University of Illinois at Urbana–Champaign, Urbana, Illinois 61801, United States

<sup>§</sup>Department of Civil and Environmental Engineering, Colorado School of Mines, Golden, Colorado 80401, United States

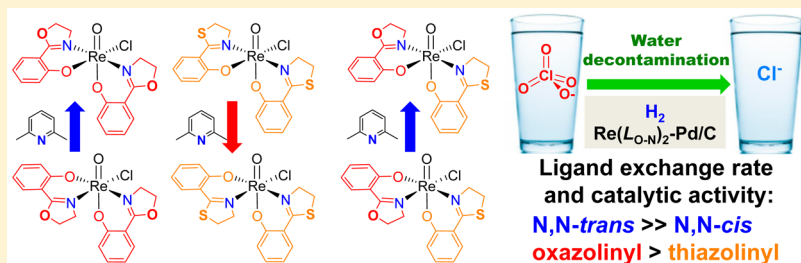
<sup>||</sup>Department of Chemistry and Biochemistry, The Ohio State University, Columbus, Ohio 43210, United States

<sup>⊥</sup>Pure Storage Inc., Mountain View, California 94041, United States

<sup>#</sup>Department of Chemistry and School of Chemical Engineering, Purdue University, West Lafayette, Indiana 47907, United States

<sup>∇</sup>Department of Civil, Architectural, and Environmental Engineering, University of Texas at Austin, Austin, Texas 78712, United States

## Supporting Information



**ABSTRACT:** This study develops synthetic strategies for N,N-*trans* and N,N-*cis* Re(O)(L<sub>O-N</sub>)<sub>2</sub>Cl complexes and investigates the effects of the coordination spheres and ligand structures on ancillary ligand exchange dynamics and catalytic perchlorate reduction activities of the corresponding [Re(O)(L<sub>O-N</sub>)<sub>2</sub>]<sup>+</sup> cations. The 2-(2'-hydroxyphenyl)-2-oxazoline (Hhoz) and 2-(2'-hydroxyphenyl)-2-thiazoline (Hhtz) ligands are used to prepare homoleptic N,N-*trans* and N,N-*cis* isomers of both Re(O)(hoz)<sub>2</sub>Cl and Re(O)(htz)<sub>2</sub>Cl and one heteroleptic N,N-*trans* Re(O)(hoz)(htz)Cl. Selection of hoz/htz ligands determines the preferred isomeric coordination sphere, and the use of substituted pyridine bases with varying degrees of steric hindrance during complex synthesis controls the rate of isomer interconversion. The five corresponding [Re(O)(L<sub>O-N</sub>)<sub>2</sub>]<sup>+</sup> cations exhibit a wide range of solvent exchange rates (1.4 to 24,000 s<sup>-1</sup> at 25 °C) and different L<sub>O-N</sub> movement patterns, as influenced by the coordination sphere of Re (*trans/cis*), the noncoordinating heteroatom on L<sub>O-N</sub> ligands (O/S), and the combination of the two L<sub>O-N</sub> ligands (homoleptic/heteroleptic). Ligand exchange dynamics also correlate with the activity of catalytic reduction of aqueous ClO<sub>4</sub><sup>-</sup> by H<sub>2</sub> when the Re(O)(L<sub>O-N</sub>)<sub>2</sub>Cl complexes are immobilized onto Pd/C. Findings from this study provide novel synthetic strategies and mechanistic insights for innovations in catalytic, environmental, and biomedical research.

## INTRODUCTION

Oxorhenium complexes have been recognized as versatile catalysts for a series of reactions used in synthetic chemistry<sup>1</sup> as well as energy and environmental related applications.<sup>2</sup> The complexes of <sup>186</sup>Re and <sup>188</sup>Re isotopes have been developed as radiopharmaceuticals for tumor imaging and radionuclide therapy.<sup>3</sup> Fluorescent chemosensing for Re in cells has also been developed based on oxorhenium(V) coordination chemistry.<sup>4</sup> Monoanionic bidentate L<sub>O-N</sub> ligands (e.g.,

salicylimine, 8-hydroxyquinoline, picolinic acid, etc.) and tetradentate L<sub>O-N-N-O</sub> ligands (e.g., *salen* and *salan*) with tunable steric and electronic properties have been widely used to prepare Re(O)(L<sub>O-N</sub>)<sub>2</sub>X<sup>5</sup> and Re(O)(L<sub>O-N-N-O</sub>)X<sup>6</sup> (X = Cl, Br, alkyl and alkoxide in neutral complexes, or X = H<sub>2</sub>O, CH<sub>3</sub>CN, etc. in cationic complexes). Of particular note, the

Received: December 22, 2015

naturally occurring 2-(2'-hydroxyphenyl)-2-oxazoline (*Hhoz*) structure originally identified in microbial siderophores<sup>7</sup> gives the  $\text{Re}(\text{O})(\text{hoz})_2\text{X}$  complex diverse catalytic activities, including perchlorate reduction,<sup>8</sup> hydrosilylation,<sup>9</sup>  $\text{H}_2$  production from organosilanes,<sup>10</sup> condensation between biomass-derived polyols and aldehydes,<sup>11</sup> and C–H activation.<sup>12</sup>

Advancement of oxorhenium chemistry has provided insights that can be applied to address major environmental and energy challenges. Perchlorate ( $\text{ClO}_4^-$ ) is a potent competitive inhibitor of the thyroid sodium-iodide symporter.<sup>13</sup> This highly inert anion has been widely detected in contaminated water supplies<sup>14</sup> and agricultural products.<sup>15</sup> A nationwide regulation of  $\text{ClO}_4^-$  in drinking water by the U.S. EPA is pending.<sup>16</sup> Our research team developing innovative water treatment technologies has immobilized  $\text{Re}(\text{O})(\text{hoz})_2\text{Cl}$  in Pd/C to prepare a novel biomimetic heterogeneous catalyst,<sup>17</sup> in which oxorhenium single sites reduce  $\text{ClO}_4^-$  anions via oxygen atom transfer (OAT, a two-electron transfer process),<sup>18</sup> and  $\text{Pd}^0$  nanoparticles transfer electrons from exogenous  $\text{H}_2$  to sustain the catalytic cycle between  $\text{Re}^{\text{V}}$  and  $\text{Re}^{\text{VII}}$ . At room temperature, this  $\text{Re}(\text{hoz})_2$ -Pd/C catalyst enables rapid reduction of  $\text{ClO}_4^-$  by  $\text{H}_2$  into  $\text{Cl}^-$  and  $\text{H}_2\text{O}$ , exhibiting much higher activity than other reported chemical reduction methods under water treatment conditions.<sup>17a</sup> Therefore, further development of oxorhenium complexes and the corresponding transformation into heterogeneous functional materials show great promise for addressing environmental, health, and energy challenges.

During our initial efforts synthesizing  $\text{Re}(\text{O})(\text{hoz})_2\text{Cl}$  following literature methods, we obtained a mixture of two  $\text{Re}(\text{O})(\text{hoz})_2\text{Cl}$  isomers showing different  $\text{ClO}_4^-$  reduction activity. After laborious isolation efforts, we characterized the two isomers as *N,N-trans* (**2a**) and *N,N-cis* (**2b**) (Figure 1), the

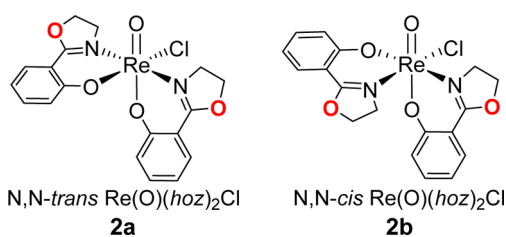


Figure 1. Previously reported  $\text{Re}(\text{O})(\text{hoz})_2\text{Cl}$  isomers.

former showing much higher  $\text{ClO}_4^-$  reduction activity than the latter.<sup>19</sup> Recently, Schachner et al.<sup>20</sup> also reported on the isolation and variable homogeneous  $\text{ClO}_4^-$  reduction activities of **2a** and **2b**. Isomerism is a frequently encountered phenomenon during the synthesis of  $\text{Re}(\text{O})(\text{L}_{\text{O-N}})_2\text{X}$  complexes, which have six possible configurations (Figure 2).<sup>5b</sup> The number of literature reported *N,N-trans*  $\text{Re}(\text{O})(\text{L}_{\text{O-N}})_2\text{X}$  structures (type A)<sup>5a,b,d,e,j</sup> are much less than *N,N-cis* structures (type B).<sup>5b–i</sup> No examples of type C or D have been reported, probably due to the *trans* influence of the oxo group. Multiple examples of the  $\text{C}_2$ -symmetric structure (type E, X = OMe or  $\text{OH}_2$ )<sup>21</sup> have been documented, while only one example of the  $\text{C}_3$ -symmetric structure (type F, X = Cl)<sup>22</sup> has been observed. However, except for the single case of  $\text{Re}(\text{O})(\text{hoz})_2\text{Cl}$  isomers, there has been no other study comparing the effects of isomeric coordination sphere on spectroscopic and catalytic properties of  $\text{Re}(\text{O})(\text{L}_{\text{O-N}})_2\text{X}$  complexes.

Synthetic challenges might be a major factor hindering isomer-specific investigations. Strategies for controlling  $\text{Re}(\text{O})$ -

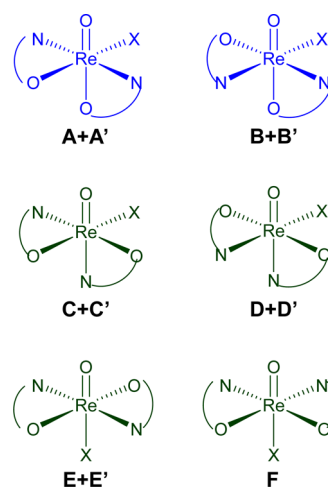


Figure 2. Possible structures of  $\text{Re}(\text{O})(\text{L}_{\text{O-N}})_2\text{X}$  isomers. Prime indicates an enantiomer.

( $\text{L}_{\text{O-N}})_2\text{X}$  isomerization, especially for type A and B, remain largely unexplored despite its importance in mechanistic study and catalyst design. In practice, synthetic procedures yielding a mixture of isomers create various difficulties in product isolation, adding challenges to structural determination and subsequent investigation on reaction mechanisms and the structure–activity relationship. Furthermore, failure to control isomeric structure might yield less active isomers, thus lowering the cost-effectiveness of catalyst preparation. Therefore, it is imperative to identify the mechanisms controlling isomer formation and interconversion, and to establish facile methods that selectively afford complex products with the desired coordination sphere.

Herein, we report a systematic investigation of *N,N-trans* and *N,N-cis*  $\text{Re}(\text{O})(\text{L}_{\text{O-N}})_2\text{Cl}$  isomers covering the following aspects: formation and interconversion during synthesis, ligand exchange dynamics, and catalytic  $\text{ClO}_4^-$  reduction activities. First, we identify the formation mechanism of  $\text{Re}(\text{O})(\text{hoz})_2\text{Cl}$  (designated OO for the noncoordinating heteroatom on the N-containing ring) isomers (*N,N-trans* **2a** and *N,N-cis* **2b**). A novel synthetic strategy is developed, which uses pyridine bases with varying levels of steric hindrance to control the conversion of **2b** to the desired and thermodynamically favored **2a**. Findings from this work also provide revised structural and mechanistic interpretations of data presented in previous reports.<sup>5e,20,23</sup> Next, to generalize the isomerism–property relationship, we extended the  $\text{L}_{\text{O-N}}$  ligand selection from *Hhoz* to *Hhtz* (2-(2'-hydroxyphenyl)-2-thiazoline). Surprisingly, ligand modification of the noncoordinating heteroatom from O to S resulted in a reversed thermodynamic preference of *N,N-cis*  $\text{Re}(\text{O})(\text{htz})_2\text{Cl}$  (SS) over the *N,N-trans* SS isomer. Finally, hybridization of *hoz* and *htz* in a single Re complex (OS) led to the selective preparation of *N,N-trans*  $\text{Re}(\text{O})(\text{hoz})_{\text{eq}}(\text{htz})_{\text{ax}}\text{Cl}$ . Comparison among the five  $\text{Re}(\text{O})(\text{L}_{\text{O-N}})_2\text{Cl}$  structures identified significantly different behaviors with respect to ligand exchange dynamics, which are correlated with catalytic  $\text{ClO}_4^-$  reduction activities.

## RESULTS

**Controlled Synthesis of *N,N-trans* and *N,N-cis*  $\text{Re}(\text{O})(\text{hoz})_2\text{Cl}$  (OO) Complexes.** The  $\text{Re}(\text{O})(\text{hoz})_2\text{Cl}$  isomers **2a** and **2b** were initially obtained following a previously reported method,<sup>23a</sup> where a  $\text{Re}(\text{O})(\text{OPPh}_3)(\text{SM}_2)\text{Cl}_3$  precursor (**1**), 2

equiv of *Hhoz* ligand, and a stoichiometric amount of 2,6-Me<sub>2</sub>Py base (for scavenging HCl) were heated in refluxing ethanol for 3 h. As determined by <sup>1</sup>H NMR, the product contained **2a** and **2b** at a 63:37 ratio. **2a** was purified by three rounds of recrystallization from CH<sub>2</sub>Cl<sub>2</sub>/pentane. **2b** was enriched in the mother liquor and isolated by silica gel chromatography using EtOAc as eluent, while **2a** tailed in the column. ORTEP diagrams and crystal data of **2a** and **2b** obtained by our efforts are provided in Figure S1, Table S1, and Table S2 in Supporting Information. We noted here that we provide a different **2b** crystal structure (crystallized with toluene) as a higher quality alternative to that recently reported by Schachner et al.,<sup>20</sup> which contained structural problems with the model showing poor displacement ellipsoids and high level CIFCheck warnings. In comparison, Schachner et al.<sup>20</sup> followed an earlier synthesis method<sup>8</sup> without using 2,6-Me<sub>2</sub>Py, and obtained a roughly 50:50 mixture of the two isomers regardless of solvents and Re precursors used during synthesis. In their report, **2a** precipitated out of ethanol, and **2b** was collected from the mother liquor and purified by Soxhlet extraction with diethyl ether to remove the residual **2a**. Because these early approaches are very laborious, we aimed to develop a convenient and generalized methodology for isomer-specific synthesis of Re(O)(L<sub>O-N</sub>)<sub>2</sub>Cl complexes, which would benefit a broad range of oxorhenium chemistry study.

The discrepancy of the isomer ratio yielded from our early approach (63:37) and from the approach by Schachner et al.<sup>20</sup> (50:50) suggested that **2a** and **2b** might be subject to interconversion. Thus, we monitored product formation at selected time intervals and found that **1** was quickly converted to an ~1:1 mixture of **2a** and **2b** within 10 min of initiating the reaction but that prolonged heating slowly converted **2b** into **2a** (Table 1, entries 1 to 4). DFT calculations indicate that **2a** has a lower Gibbs free energy than **2b** ( $\Delta G = -0.59$  kcal mol<sup>-1</sup> at 78 °C in ethanol; more detailed results are provided in Table S3). Since both isomers have limited solubility in ethanol, we first attempted to accelerate the conversion by dissolution in chloroform. However, no conversion was observed in chloroform, suggesting the need for a polar reaction environment. Instead, the conversion in ethanol was accelerated by adding excess 2,6-Me<sub>2</sub>Py (Table 1, entries 5 to 8). Direct mixing of **1** with 2,6-Me<sub>2</sub>Py, which is commonly used as a sterically hindered noncoordinating base, resulted in a dark brown product. Therefore, the two methyls do not completely block coordination with Re (2,6-Me<sub>2</sub>Py coordination with Os<sup>24</sup> and Pt<sup>25</sup> have also been reported), and it appears that this coordination plays a key role in the isomer interconversion.

Pyridine bases with a variety of substitutions were evaluated to probe the structural effects on Re isomer interconversion. Nonsubstituted Py resulted in some uncharacterized products attributed to its strong binding with Re (Table 1, entries 9 and 10). Substitution with one methyl in 2-MePy destabilized the Py-Re binding and yielded **2a** and **2b** but did not promote isomer interconversion (entries 11 and 12). The 2,4-Me<sub>2</sub>Py, with a higher electron density on N but the same steric hindrance of coordination as 2-MePy, achieved even faster isomer interconversion than 2,6-Me<sub>2</sub>Py (entries 13 and 14). Thus, both partial steric hindrance and enhanced electron density on the coordinating Py are important for catalyzing the isomer conversion. As expected, the bulky 2,6-*t*Bu<sub>2</sub>Py<sup>26</sup> showed no effect on the conversion (entries 15 and 16). A mechanism for Py-facilitated isomer interconversion from **2b** to **2a** is proposed in the Supporting Information (Scheme S1).

Table 1. Formation of Re(O)(*hoz*)<sub>2</sub>Cl Isomers **2a** and **2b**<sup>a</sup>

entry	base	base amount <sup>b</sup>	time	2a:2b <sup>c</sup>
1		1	10 min	53:47
2			3 h	63:37
3			18 h	77:23
4			12 h <sup>d</sup>	52:48 <sup>d</sup>
5		2.5	10 min	54:46
6			1 h	60:40
7			3 h	93:7
8			24 h	100:0
9		2.5	10 min	N/A <sup>e</sup>
10			1 h	N/A <sup>e</sup>
11		2.5	10 min	50:50
12			1 h	52:48
13		2.5	10 min	57:43
14			1 h	72:28
15		2.5	10 min	49:51
16			1 h	51:49

<sup>a</sup>Reaction conditions: **1** (20 mg, 0.031 mmol), *Hhoz* (10.1 mg, 0.062 mmol), ethanol (1.2 mL), and reflux (80 °C oil bath). <sup>b</sup>In molar equivalents relative to *Hhoz*. <sup>c</sup>Ratio determined with <sup>1</sup>H NMR (500 MHz, CDCl<sub>3</sub>) from integration area of  $\delta$  7.90 (**2a**) and  $\delta$  7.81 (**2b**) doublets. <sup>d</sup>Reaction at room temperature. <sup>e</sup>Unknown products besides **2a** and **2b** also formed.

A simple method to exclusively yield **2a** was thus established by using an excess amount of 2,4- or 2,6-Me<sub>2</sub>Py and heating for 48 h. Meanwhile, **2b** could not be prepared higher than 50% yield when a base was used. An attempt to exclusively synthesize **2b** without adding base was unsuccessful, but a new product, [H<sub>2</sub>*hoz*][Re(O)(*hoz*)Cl<sub>3</sub>] (**3**, Figure 3), was obtained. Results agree with Lobmaier et al.<sup>22</sup> who synthesized Re(O)(L<sub>O-N</sub>)<sub>2</sub>Cl complexes from another commonly used precursor, [NBu<sub>4</sub>][Re(O)Cl<sub>4</sub>]; reaction with 2 equiv of bis(alkyl/aryl)-(2'-pyridyl)alcoholate ligands without added base resulted in the formation of [Re(O)(L<sub>O-N</sub>)Cl<sub>3</sub>]<sup>-</sup> and [H<sub>2</sub>L<sub>O-N</sub>]<sup>+</sup>, and 4 equiv of HL<sub>O-N</sub> were necessary to synthesize Re(O)(L<sub>O-N</sub>)<sub>2</sub>Cl, where 2 equiv of HL<sub>O-N</sub> were sacrificed as a base. These findings contrast the earlier reports,<sup>8,20</sup> where only 2 equiv of *Hhoz* were used without added base to synthesize the mixture of **2a** and **2b**. The results also suggest that [Re(O)(*hoz*)Cl<sub>3</sub>]<sup>-</sup> is an intermediate that reacts with a second *hoz* ligand to yield **2a** and **2b** with equal probability. To verify this mechanism, we synthesized [H*t*Bu<sub>2</sub>Py][Re(O)(*hoz*)Cl<sub>3</sub>] (**4**) from **1** with stepwise and slow addition of 1 equiv of *Hhoz* and 1 equiv of 2,6-*t*Bu<sub>2</sub>Py base (Figure 3). Subsequent reaction of **4** with a second equivalent of *Hhoz* and 2,6-*t*Bu<sub>2</sub>Py afforded **2a** and **2b** in 1:1 ratio. Thus, the highest yield of **2b** remains limited to 50%. The initial 1:1 formation of two isomers is kinetically controlled since **2a** is thermodynamically favored over **2b**, but the exact mechanism remains unclear.

**Synthesis of N,N-*trans* and N,N-*cis* Re(O)(*htz*)<sub>2</sub>Cl (SS) Isomers with Reversed Formation Preference.** Previously, the coordination sphere of Re(O)(*htz*)<sub>2</sub>Cl was reported as N,N-*cis*.<sup>23b</sup> The success on the Re(O)(*hoz*)<sub>2</sub>Cl isomer synthesis motivated us to obtain the corresponding N,N-*trans* Re(O)(*htz*)<sub>2</sub>Cl structure, which would enable the comparison of ligand effects with the same Re coordination sphere. Thus, we

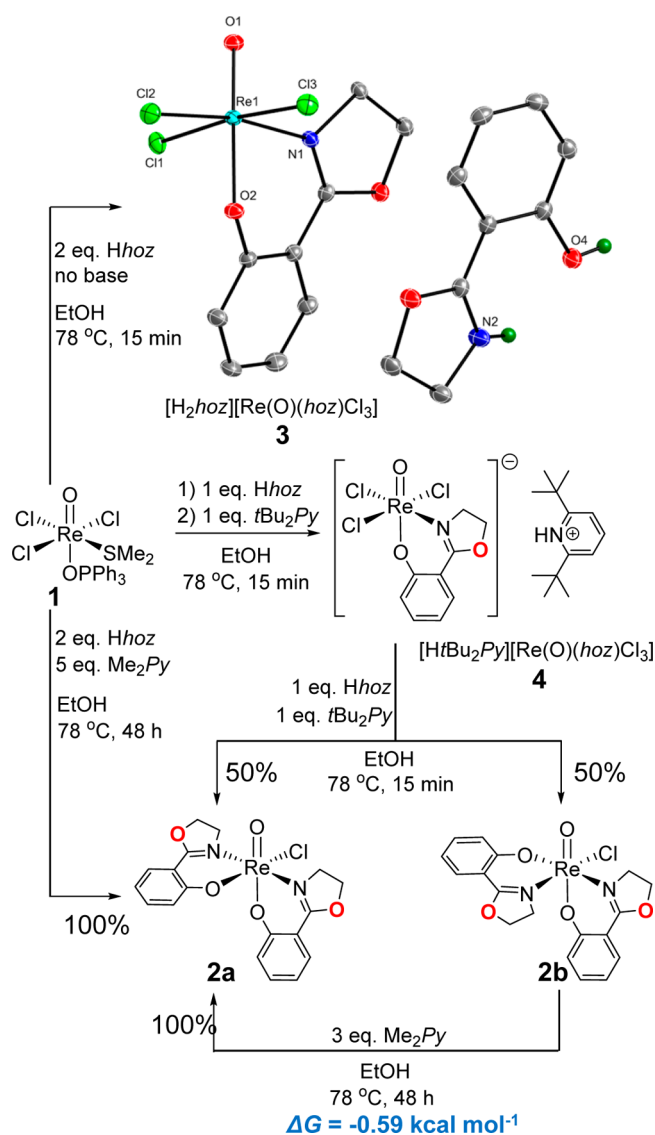


**Figure 3.** Formation and conversion of *hoz*-coordinated Re complex products. Structure of **3** is shown with a 35% probability thermal ellipsoid ORTEP diagram. DFT-calculated relative Gibbs free energy (in EtOH at 78 °C) is provided.

targeted the synthesis of *N,N-trans*  $\text{Re}(\text{O})(\text{htz})_2\text{Cl}$  (**5a**) following the method of using excess *Me*<sub>2</sub>*Py* that exclusively yielded the *N,N-trans* **2a** and isolation of *N,N-cis*  $\text{Re}(\text{O})(\text{htz})_2\text{Cl}$  (**5b**) from the initial 1:1 isomer mixture by chromatographic separation.

Again, two isomers initially formed in an approximately 1:1 ratio after 15 min (Figure 4). Consistent with the isolation of **2b**, **5b** could be selectively eluted with silica gel chromatography, and crystallography confirmed the *N,N-cis* structure. Surprisingly, ligand shift from *hoz* to *htz* reversed the direction of isomer interconversion during prolonged heating with excess *Me*<sub>2</sub>*Py*. After 48 h, the initially formed **5a** converted completely to **5b**, consistent with the lower Gibbs free energy calculated for the latter. As a result, isolation of **5a** (confirmed by crystallography to be the *N,N-trans* structure) from the 1:1 isomer mixture required multiround extraction with chloroform (where the solubility of **5a** is much higher than that of **5b**).

**Synthesis of *N,N-trans*  $\text{Re}(\text{O})(\text{hoz})(\text{htz})\text{Cl}$  (**5S**).** The competition between *hoz* and *htz* in determining *trans/cis*

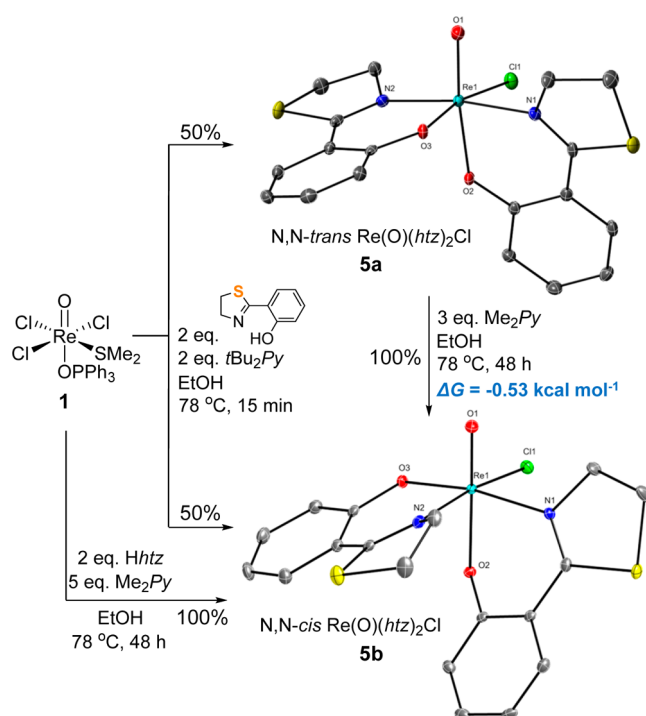


**Figure 4.** Formation and conversion of  $\text{Re}(\text{O})(\text{htz})_2\text{Cl}$  isomers (structures shown with 35% probability thermal ellipsoid ORTEP diagrams). DFT-calculated relative Gibbs free energy (in EtOH at 78 °C) is provided.

preference motivated us to hybridize the two ligands in a single heteroleptic Re complex. As illustrated in Figure 5, two intermediates,  $[\text{Re}(\text{O})(\text{hoz})\text{Cl}_3]^-$  (**4**) and  $[\text{Re}(\text{O})(\text{htz})\text{Cl}_3]^-$  (**6**), were first prepared from **1**. Both structures have the  $L_{\text{O-N}}$  ligand occupying the axial position along the oxo bond. After **4** and **6**, respectively, reacted with a second *Hhtz* or *Hhoz*, we were surprised to find that regardless of the *hoz/htz* addition sequence the final product was *N,N-trans*  $\text{Re}(\text{O})(\text{hoz})_{\text{eq}}(\text{htz})_{\text{ax}}\text{Cl}$  (**7a**). DFT calculations suggest that **7a** is more stable in comparison with the other three possible isomeric structures **7b**, **7c**, and **7d** (Figure 5). Notably, although *hoz* initially occupied the axial position in **4**, it shifted to the equatorial position when *htz* was added. This implies that the mechanism for the initial 1:1 formation of **2a** and **2b**, as well as **5a** and **5b**, could be more complicated than a previously conceived process, where two equatorial Cl ligands in **4** and **6** were substituted by the second  $L_{\text{O-N}}$  while the axial  $L_{\text{O-N}}$  remained static.

With both ligand hybridization sequences for the synthesis, **7a** was already dominant within 15 min after adding the second  $L_{\text{O-N}}$  equivalent to **4** or **6**. A minor product (~17%) observed at 15 min gradually disappeared over the following 48 h when heating with excess *Me*<sub>2</sub>*Py*. Because of the low solubility of the hybrid ligand complex products, the minor species was not isolated. However, based on the observed preference of *htz* at the axial position and the DFT calculation results (Figure 5), *N,N-cis*  $\text{Re}(\text{O})(\text{hoz})_{\text{eq}}(\text{htz})_{\text{ax}}\text{Cl}$  (**7c**) is the most probable structure for this transient product. In addition, another set of <sup>1</sup>H NMR peaks (see NMR spectra in Supporting Information) was observed in the  $\text{CDCl}_3$  solution of recrystallized **7a**. However, cationic **7a**<sup>+</sup> prepared from the same batch of **7a** showed high purity (see below). Thus, an isomerization occurred in the  $\text{CDCl}_3$  solution of **7a**, but the structure of

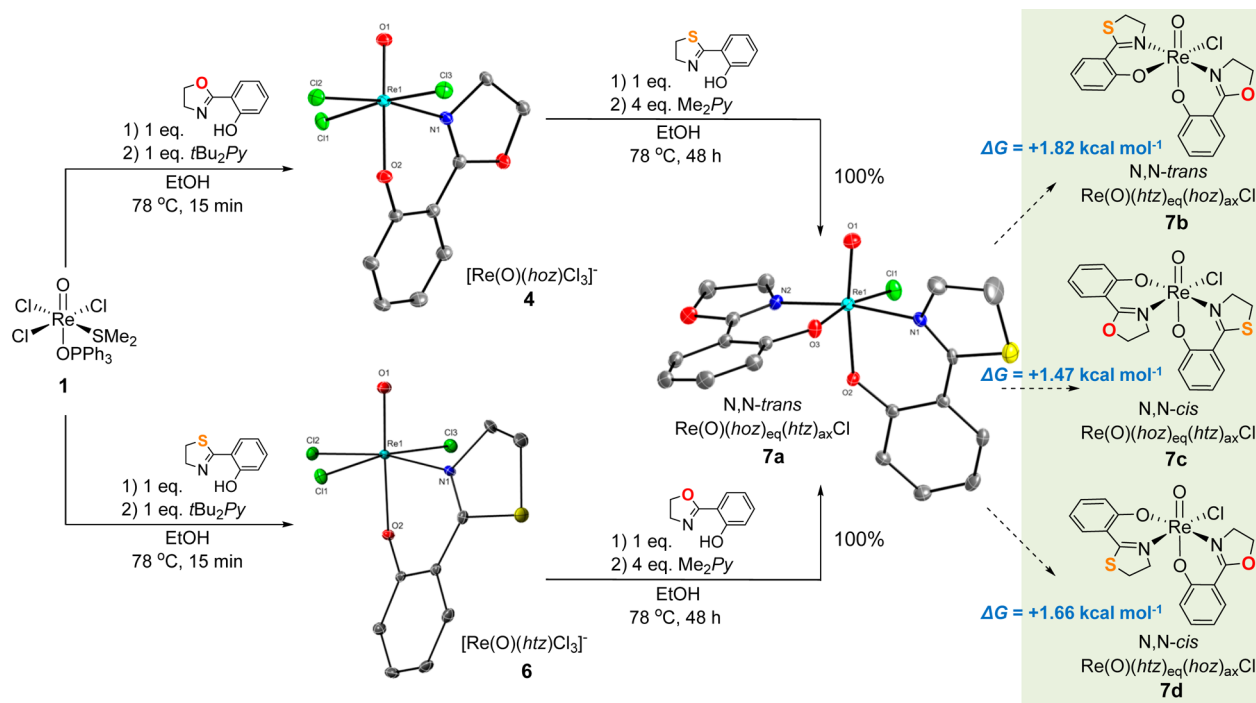


**Figure 5.** Synthesis of  $\text{Re}(\text{O})(\text{hoz})(\text{htz})\text{Cl}$ . Structure of **7a** and the anionic part of **4** (the same as **3**) and **6** are shown with 35% probability thermal ellipsoid ORTEP diagrams. Three theoretical isomer structures are shown in the green area. DFT-calculated relative Gibbs free energies (in EtOH at  $78^\circ\text{C}$ ) are provided.

this isomer and related conversion mechanism remain unclear. The OS hybrid design reversed the *N,N-cis* isomer preference encountered during SS complex synthesis.

**Ligand Exchange Dynamics of Homoleptic  $[\text{Re}(\text{O})(\text{hoz})_2]^+$  and  $[\text{Re}(\text{O})(\text{htz})_2]^+$  Cations.** First, **2a** and **2b** were converted into cationic  $[\text{Re}(\text{O})(\text{hoz})_2]^+$  structures (**2a<sup>+</sup>** and **2b<sup>+</sup>**, respectively) with  $\text{AgOTf}$  in  $\text{CD}_3\text{CN}$ . Compared to  $\text{Re}(\text{O})(\text{hoz})_2\text{Cl}$  precursors, the cationic species showed darker green colors (see Supporting Information for UV-vis spectra). According to the electronic structure analysis by Machura et al.,<sup>5b,j,27</sup> the HOMO of  $\text{Re}(\text{O})(L_{\text{O-N}})_2\text{X}$  complexes is a mixture of Re *d* orbitals and the  $\pi$  orbitals of both  $L_{\text{O-N}}$  and X ligands. Thus, the exchange of ligand X from  $\text{Cl}^-$  to  $\text{CH}_3\text{CN}$  led to altered energies of charge transfer from HOMO to LUMO (or higher orbitals) responsible for the visible light adsorption. At room temperature,  $^1\text{H}$  NMR showed an apparent symmetry for the two *hoz* ligands in **2a<sup>+</sup>** but not in **2b<sup>+</sup>** (Figure 6). VT NMR showed asymmetric resonances of **2a<sup>+</sup>** at lower temperature and broadened resonances of **2b<sup>+</sup>** at elevated temperature, suggesting that **2a<sup>+</sup>** has a much faster intramolecular exchange of the two *hoz* ligands than **2b<sup>+</sup>**. At  $-12.9^\circ\text{C}$ , where the coalescence of  $\delta$  7.87–8.02 resonances of **2a<sup>+</sup>** was observed, the *hoz* ligand exchange rate constant ( $k_L$ ) was calculated to be  $160\text{ s}^{-1}$  according to eq 1:

$$k_L = \frac{\pi\Delta\nu}{\sqrt{2}} \quad (1)$$

where  $\Delta\nu$  represents the separation of frequency (Hz) between the two coalescing resonances.<sup>28</sup>

We propose five-coordinate structures, upon solvent dissociation, as the intermediates (**2aI<sup>+</sup>** and **2bI<sup>+</sup>** in Figure 6) during the exchange of the two *hoz* ligands. To quantify the solvent dissociation rate, 10% (v/v)  $\text{CH}_3\text{CN}$  was added to the  $\text{CD}_3\text{CN}$  solutions of **2a<sup>+</sup>** and **2b<sup>+</sup>**. A new singlet corresponding

to Re-coordinated  $\text{CH}_3\text{CN}$  appeared ( $\delta$  2.83 for **2a<sup>+</sup>** and  $\delta$  3.07 for **2b<sup>+</sup>**, both with an integration area of 0.3 as a result of the 10% probability of  $\text{CH}_3\text{CN}$  coordination; Figure 7). At room temperature, presaturation of free  $\text{CH}_3\text{CN}$  resonance at  $\delta$  1.94 caused partial suppression of the Re-coordinated  $\text{CH}_3\text{CN}$  resonance in **2a<sup>+</sup>**, supporting the dynamic exchange between Re-bound and free solvent molecules. At different temperatures (*T*), the solvent ligand exchange rate constants ( $k_S$ ) were determined according to eq 2:

$$k_S = \pi(\omega_{1/2} - \omega_0) \quad (2)$$

where  $\omega_{1/2}$  and  $\omega_0$  indicate the measured half-height line width (Hz) for resonances of Re-coordinated and free  $\text{CH}_3\text{CN}$ , respectively. Activation enthalpy ( $\Delta H^\ddagger$ ) and entropy ( $\Delta S^\ddagger$ ) of  $\text{CH}_3\text{CN}$  exchange with **2a<sup>+</sup>** and **2b<sup>+</sup>** were obtained via eq 3:<sup>28</sup>

$$\log \frac{k_S}{T} = 10.32 - \frac{\Delta H^\ddagger}{19.14T} + \frac{\Delta S^\ddagger}{19.14} \quad (3)$$

As shown in Table 2 (entries 1 and 2),  $\Delta S^\ddagger$  values are highly positive for both isomers and consistent with a dissociative mechanism. The marked difference of  $\Delta H^\ddagger$  for **2a<sup>+</sup>** and **2b<sup>+</sup>** thus derives from the step of solvent ligand dissociation from  $[\text{Re}(\text{O})(\text{hoz})_2(\text{NCCH}_3)]^+$ . The estimated  $k_S$  values for **2a<sup>+</sup>** and **2b<sup>+</sup>** at  $25^\circ\text{C}$  differ by a factor of 5,300 ( $24,000\text{ s}^{-1}$  versus  $4.5\text{ s}^{-1}$ ). The calculated  $k_S$  for **2a<sup>+</sup>** at  $-12.9^\circ\text{C}$  is  $320\text{ s}^{-1}$ , twice the *hoz* ligand exchange rate  $k_L$  ( $160\text{ s}^{-1}$ ) measured with the coalescence approach (eq 1). This validates the proposed *hoz* exchange mechanism involving solvent dissociation (Figure 6); either retention or exchange of the axial/equatorial position of the two *hoz* takes 50% probability. The *hoz* ligand exchange in **2a<sup>+</sup>** does not alter the Re complex structure, whereas ligand exchange in **2b<sup>+</sup>** yields the enantiomeric **2b<sup>+</sup>**. Results shown here correct a previously interpreted structure for **2a<sup>+</sup>** in  $\text{CD}_3\text{CN}$  as  $C_2$ -symmetric with a  $\text{H}_2\text{O}$  coordinated *trans* to the

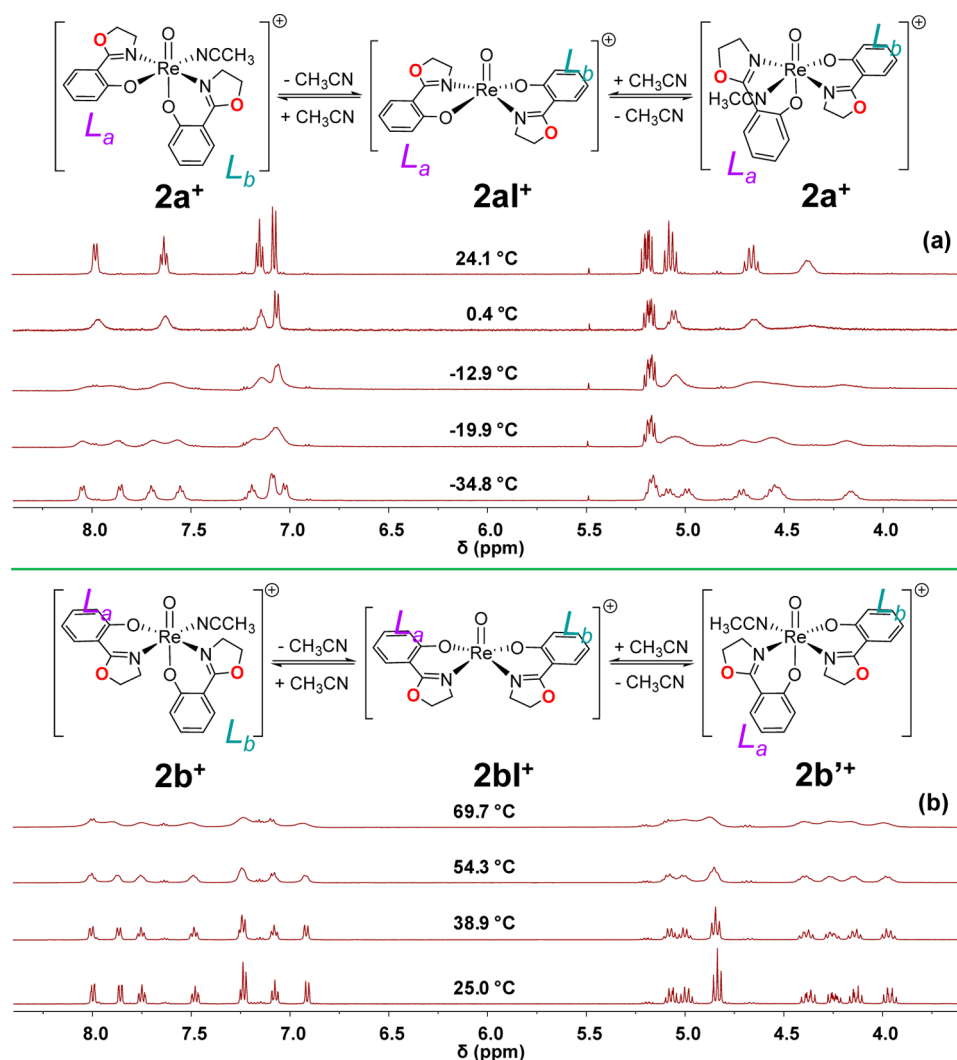


Figure 6. VT  $^1\text{H}$  NMR (500 MHz,  $\text{CD}_3\text{CN}$ ) spectra and proposed ligand exchange mechanisms for (a)  $2\text{a}^+$  and (b)  $2\text{b}^+$ .

oxo group,<sup>20,23</sup> although such a structure was obtained upon crystallization in water-containing solvent (Figure S2). We also note that the previously proposed interconversion between two *N,N-trans* cationic enantiomers<sup>5e,20</sup> is less likely because enantiomerization of  $2\text{a}^+$  into  $2\text{a}'^+$  requires complicated physical contortions.

The varying tendency for ligand dissociation from  $2\text{a}^+$  and  $2\text{b}^+$  does not only apply to the neutral solvent. When  $[\text{Re}(\text{O})(\text{hoz})_2]^+$  was prepared from  $\text{Re}(\text{O})(\text{hoz})_2\text{Cl}$  isomers,  $\text{AgCl}$  precipitation was immediately observed upon addition of  $\text{AgOTf}$  to the suspension of  $2\text{a}$  but was delayed by several seconds when the silver salt was added to  $2\text{b}$ . Density functional theory (DFT) calculations performed by Schachner et al.<sup>20</sup> suggested a 3–4  $\text{kcal mol}^{-1}$  higher energy required to remove  $\text{Cl}^-$  allowed for convenient chromatographic isolation of  $2\text{b}$  from  $2\text{a}$  ( $2\text{b}$  can be exclusively synthesized, so the chromatography isolation is not needed). Using pure ethyl acetate,  $2\text{b}$  was readily eluted as a narrow green band ( $R_f = 0.7$ ). In contrast, the facile dissociation of  $2\text{a}$  yields  $\text{Cl}^-$  and  $2\text{a}^+$ , which is electrostatically attracted to the anionic silica gel, resulting in delayed elution with significant tailing even after switching the eluent to pure methanol.

The preparation of  $5\text{a}^+$  from  $5\text{a}$  with  $\text{AgOTf}$  was rapid at room temperature, whereas the preparation of  $5\text{b}^+$  required heating at 80 °C for at least 2 h. Thus, replacement of the noncoordinating heterocyclic O with S slows  $\text{Re}-\text{Cl}$  dissociation. VT NMR measurement also showed generally slower solvent ligand dissociation from *htz*-coordinated structures than from the corresponding *hoz*-coordinated structures. At room temperature,  $5\text{a}^+$  showed only two broad resonances in the aliphatic region but gradually resolved into eight resonances as temperature was lowered (Figure 8). The  $\text{CH}_3\text{CN}$  dissociation rate constants at 25 °C for  $5\text{a}^+$  and  $5\text{b}^+$  were measured (Figure S3; Table 2, entries 3 and 4) and found to be smaller than those for  $2\text{a}^+$  and  $2\text{b}^+$ , respectively. The alteration of O to S led to a 3–4  $\text{kcal mol}^{-1}$  increase in  $\Delta H^\ddagger$  of  $\text{CH}_3\text{CN}$  dissociation from  $\text{Re}$ .

**Ligand Exchange Dynamics of Heteroleptic  $[\text{Re}(\text{O})(\text{hoz})(\text{htz})]^+$  Cation.**  $7\text{a}^+$  was prepared from  $7\text{a}$  in a similar way to the preparation of  $2\text{a}^+$  and  $5\text{a}^+$ . VT NMR showed markedly different behavior of this heteroleptic  $[\text{Re}(\text{O})(\text{hoz})(\text{htz})]^+$  cation in comparison to that of the homoleptic  $[\text{Re}(\text{O})(\text{hoz})_2]^+$  and  $[\text{Re}(\text{O})(\text{htz})_2]^+$  cations. At room temperature, an asymmetric set of resonances was observed (Figure 9a).

At first glance, *N,N-trans*  $7\text{a}^+$  seems to behave similarly to the two *N,N-cis*  $2\text{b}^+$  and  $5\text{b}^+$ . However, no  $\text{Re}$ -coordinated  $\text{CH}_3\text{CN}$

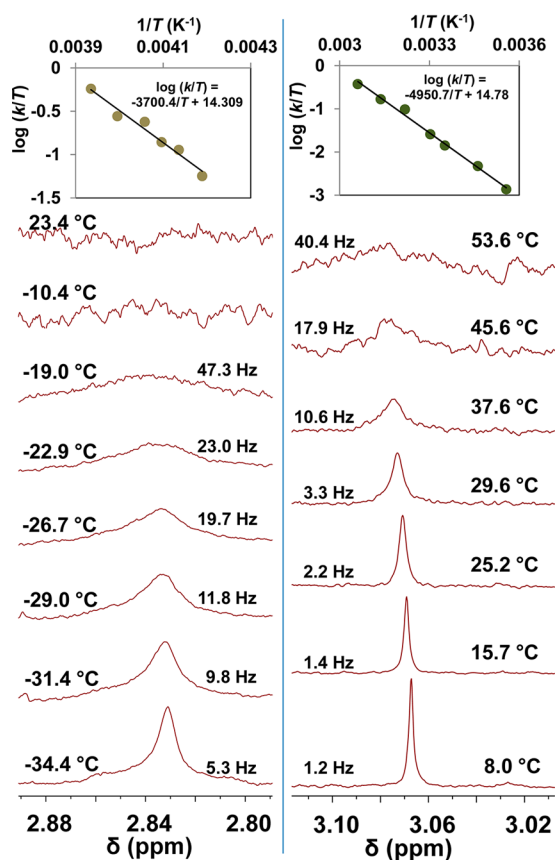


**Figure 7.** VT  $^1\text{H}$  NMR (500 MHz,  $\text{CD}_3\text{CN}$ ) spectra (half-height line width shown) of  $\text{CH}_3\text{CN}$  coordinated in  $2\text{a}^+$  (left) and  $2\text{b}^+$  (right). Inset plots: model fitting for measured solvent exchange rate ( $k_s$ ) and temperature ( $T$ ).

**Table 2.** Calculated Activation Enthalpy and Entropy, and Rate Constant at 25 °C for the Solvent Ligand Exchange between  $[\text{Re}(\text{O})(L_{\text{O-N}})_2(\text{NCCH}_3)]^+$  and the Free  $\text{CH}_3\text{CN}$  Solvent

entry	cation	$\Delta H^\ddagger$ (kJ mol $^{-1}$ ) <sup>a</sup>	$\Delta S^\ddagger$ (J K $^{-1}$ mol $^{-1}$ ) <sup>a</sup>	$k_s$ (s $^{-1}$ ) at 25 °C
1	$2\text{a}^+$	$70.8 \pm 6.4$	$76.3 \pm 26.2$	$2.4 \times 10^4$
2	$2\text{b}^+$	$94.8 \pm 3.3$	$85.4 \pm 10.9$	4.5
3	$5\text{a}^+$	$75.2 \pm 0.9$	$78.1 \pm 3.6$	$5.0 \times 10^3$
4	$5\text{b}^+$	$98.1 \pm 7.6$	$87.1 \pm 23.8$	1.4
5	$7\text{a}^+$	$62.5 \pm 1.4$	$25.1 \pm 5.7$	$1.4 \times 10^3$

<sup>a</sup>Errors represent 95% confidence intervals.

singlet was observed after the 10%  $\text{CH}_3\text{CN}$  addition (Figure S4), indicating a rapid solvent exchange at room temperature. At lower temperature, the *hoz*/*htz* resonances first broadened and then turned into sharp peaks with slightly altered chemical shifts (Figure 9a). Meanwhile, a gradually sharpened Re-coordinated  $\text{CH}_3\text{CN}$  singlet at  $\delta$  2.75 was also observed (Figure S4), and the calculated  $\Delta H^\ddagger$  and  $\Delta S^\ddagger$ , as well as  $k_s$  at 25 °C (Table 2, entry 5) were the lowest among the three *N,N*-*trans* cations. Comparison of  $^1\text{H}$  NMR spectra of the three *N,N*-*trans* cations at the lowest temperature examined (Figure 9b) suggests that the axial *htz* and equatorial *hoz* in the OS hybrid  $7\text{a}^+$  have very similar chemical environments to those of the corresponding *htz* and *hoz* ligands in  $5\text{a}^+$  and  $2\text{a}^+$ . Examination of the  $^1\text{H}$  NMR spectrum for  $7\text{a}^+$  at  $-34.4$  °C identified a small amount of equatorial *htz* and axial *hoz* (Figure S5), indicating the presence of  $\sim 2\%$   $7\text{b}^+$  in the solution of  $7\text{a}^+$ . As the

temperature increased, the ratio of  $7\text{b}^+$  in the equilibrium was elevated, and the interconversion was accelerated, leading to the coalescence and slight shifts of the resonances (Figure 9a).

Results also suggest a  $\text{CH}_3\text{CN}$  dissociation process with reduced  $L_{\text{O-N}}$  movement around Re. While  $\text{C}_2$ -symmetric square pyramidal intermediates,  $2\text{aI}^+$  and  $5\text{aI}^+$ , are proposed for OO and SS cations (Figure 6 and Figure 8), the dominant  $7\text{aI}^+$  structure might be distorted. First, both experimental observations and DFT calculations indicate that *htz* and *hoz* have specific location preferences in the OS hybrid complex. We propose that the square pyramidal five coordinate intermediate  $7\text{aI}^{*+}$  and its further conversion to  $7\text{b}^+$  are not favored (Figure 9a). Second, the distinctively low  $\Delta S^\ddagger$  (Table 2) likely originates from the relatively reduced geometry change occurring upon solvent dissociation. The lowered  $\Delta H^\ddagger$  may also be due to the relatively reduced  $L_{\text{O-N}}$  movement. The calculated solvent exchange rate constant  $k_s$  for  $7\text{a}^+$  at 25 °C is correspondingly lowered to  $1,400$  s $^{-1}$ .

**Catalytic Perchlorate Reduction in Homogeneous and Heterogeneous Systems.** The differences in monodentate ancillary ligand dissociation of *N,N*-*trans* and *N,N*-*cis* isomers correlate with differences in rates of homogeneous catalytic  $\text{ClO}_4^-$  reduction by  $\text{Me}_2\text{S}$ , as first demonstrated by the comparison between  $2\text{a}^+$  and  $2\text{b}^+$  (Figure 10a). The proposed multistep process is illustrated in Scheme 1. The dominant Re species present in the reaction initiated with  $2\text{a}^+$  was actually the chloride form  $2\text{a}$  (Figures S6 and S7a), suggesting that the bound  $\text{Cl}^-$  is labile to exchange with  $\text{ClO}_4^-$  and  $\text{ClO}_x^-$  intermediates. In contrast, the major Re species observed in the reaction initiated with  $2\text{b}^+$  was first the sulfoxide-coordinating structure  $[\text{Re}(\text{O})(\text{hoz})_2(\text{OSR}_2)]^+$ , which slowly transitioned to the chloro structure  $2\text{b}$  as the  $\text{Cl}^-$  product built up over a period of 4 h (Figures S7b and S8). In addition, DFT calculations reported previously by Schachner et al.<sup>20</sup> suggests that, after the OAT from  $\text{ClO}_4^-$  to  $\text{Re}^{\text{V}}$ , the  $\text{ClO}_3^-$  product was much more difficult to dissociate from the oxidized *N,N*-*cis*  $[\text{Re}^{\text{VII}}(\text{O})_2(\text{hoz})_2]^+$  than from *N,N*-*trans*  $[\text{Re}^{\text{VII}}(\text{O})_2(\text{hoz})_2]^+$ . Although a quantitative model describing the multistep processes is difficult to establish, findings collectively suggest that the generally faster monodentate ligand dissociation from *N,N*-*trans* structures leads to greater reactivity with  $\text{ClO}_4^-$ . The accumulation of  $\text{Cl}^-$  in solution effectively prevents  $2\text{b}$  from dissociating into the active  $2\text{b}^+$  such that complete  $\text{ClO}_4^-$  reduction could not be achieved within 2 d. In contrast to the earlier report<sup>20</sup> where  $\text{Ph}_2\text{S}$  was used as the reductant ( $k = 1.1$  M $^{-1}$  s $^{-1}$ ),  $[\text{Re}^{\text{VII}}(\text{O})_2(\text{hoz})_2]^+$  reduction by  $\text{Me}_2\text{S}$  and  $\text{Et}_2\text{S}$  ( $k = 7500$  and  $6900$  M $^{-1}$  s $^{-1}$ , respectively) is much faster than the oxidation of  $2\text{a}^+$  by  $\text{ClO}_4^-$  and  $\text{ClO}_3^-$  ( $k = 0.45$  and  $28$  M $^{-1}$  s $^{-1}$ , respectively).<sup>23b</sup> Therefore, throughout the reaction we did not observe  $[\text{H}_2\text{hoz}]^+$ , which is indicative of the accumulation of  $[\text{Re}^{\text{VII}}(\text{O})_2(\text{hoz})_2]^+$  and subsequent decomposition to  $\text{ReO}_4^-$  and  $[\text{H}_2\text{hoz}]^+$ .<sup>17c</sup>

For aqueous heterogeneous  $\text{ClO}_4^-$  reduction,  $2\text{a}$  and  $2\text{b}$  were immobilized in Pd/C by absorption via transient dissolution in water, which is more convenient to operate than the traditional incipient wetness method in terms of protecting the heterogenized Re species from oxidation by air.<sup>17a</sup> Immobilization was accompanied by quantitative  $\text{Cl}^-$  release from both isomers. Cationic Re complexes are immobilized in activated carbon matrix via both hydrophobic and electrostatic interactions.<sup>17a</sup> As shown in Figure 10b, the resulting  $\text{Re}(\text{hoz})_2$ -Pd/C catalyst prepared from  $2\text{a}$  exhibited a 24-fold greater pseudo-first-order rate constant for  $\text{ClO}_4^-$

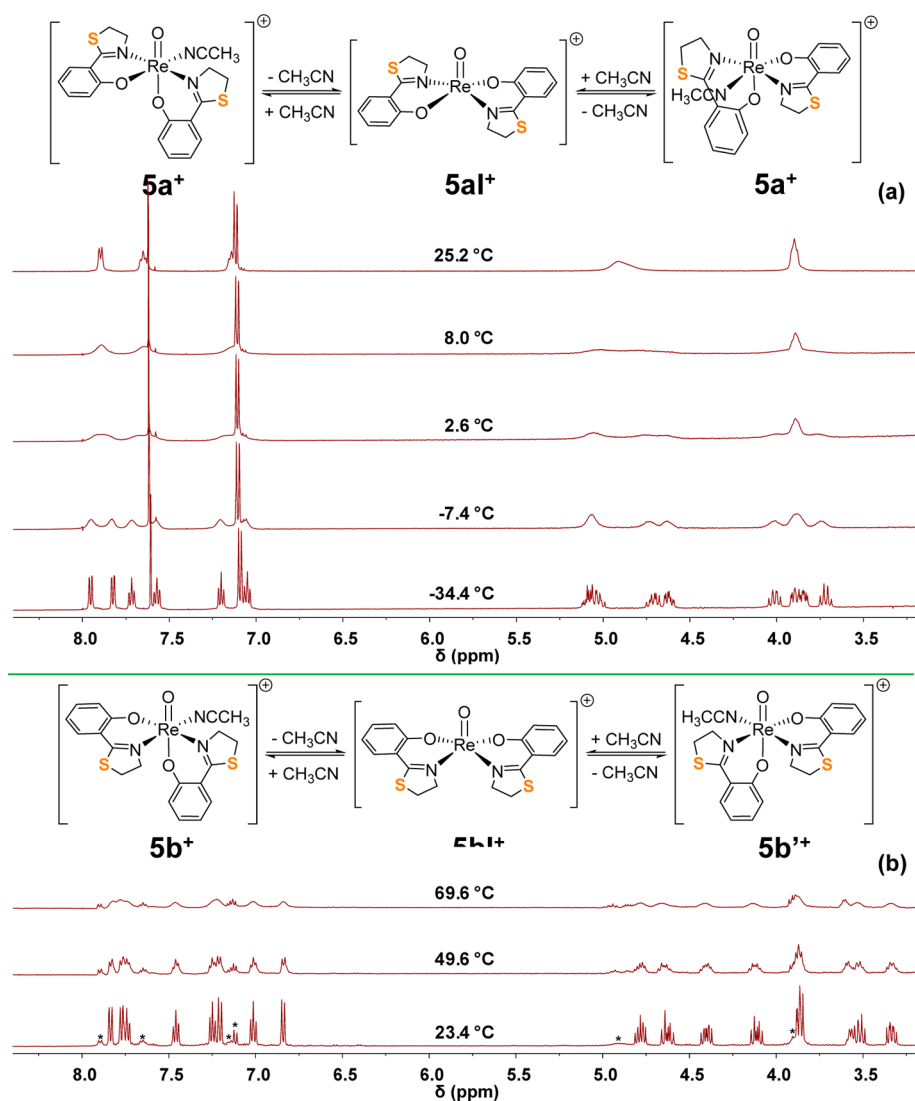


**Figure 8.** VT  $^1\text{H}$  NMR (500 MHz,  $\text{CD}_3\text{CN}$ ) spectra and proposed ligand exchange mechanism for (a)  $5\text{a}^+$  and (b)  $5\text{b}^+$ . Impurities marked with asterisks represent  $5\text{a}^+$  formed during the chloride abstraction from  $5\text{b}$  under reflux temperature.

reduction (Table 3) than that prepared from  $2\text{b}$ , in line with the general trend observed for homogeneous reactions and ligand exchange kinetics.

Homogeneous  $\text{ClO}_4^-$  reduction using  $5\text{a}^+$  and  $5\text{b}^+$  (Figure 11a) was found to be slower than the corresponding  $2\text{a}^+$  and  $2\text{b}^+$ . We note that the small amount of  $\text{ClO}_4^-$  reduction observed with  $5\text{b}^+$  is actually attributed to the presence of  $\sim 10\%$   $5\text{a}^+$  generated during the preparation of  $5\text{b}^+$  under heating (Figure 8b). Aqueous  $\text{ClO}_4^-$  reduction using  $\text{Re}(\text{htz})_2\text{-Pd/C}$  prepared from  $5\text{a}$  and  $5\text{b}$  (Figure 11b) also shows that heterogenized  $\text{Re}(\text{htz})_2$  sites provide lower activity than  $\text{Re}(\text{hoz})_2$ . Here, the heterogeneous catalyst prepared from the high purity  $N,N\text{-cis}$   $5\text{b}$  showed no activity, even though  $\text{Cl}^-$  dissociated upon immobilization in  $\text{Pd/C}$  at room temperature. These results confirm that  $N,N\text{-trans}$  structures provide substantially faster ligand dissociation and higher  $\text{ClO}_4^-$  reduction activity than  $N,N\text{-cis}$  structures, demonstrating the importance of developing effective synthetic strategies to selectively yield the more reactive  $N,N\text{-trans}$  isomers for optimum catalytic properties.

Homogeneous  $\text{ClO}_4^-$  reduction using  $7\text{a}^+$  showed similar activity with  $5\text{a}^+$  (Figure 12), whereas the heterogeneous

$\text{Re}(\text{hoz})(\text{htz})\text{-Pd/C}$  catalyst provided an activity falling between that observed for the  $\text{Re}(\text{hoz})_2\text{-Pd/C}$  and  $\text{Re}(\text{htz})_2\text{-Pd/C}$  catalysts prepared from the  $N,N\text{-trans}$  complexes (Table 3).

## DISCUSSION

**Control and Determination of the  $\text{Re}(\text{O})(\text{L}_{\text{O-N}})_2\text{Cl}$  Isomer Structure.** The isomer interconversion results for  $2\text{a}$  versus  $2\text{b}$  and  $5\text{a}$  versus  $5\text{b}$  demonstrate that alteration of the noncoordinating heteroatom in the ligand structure can reverse the relative stability of competing isomers. Earlier results of  $\text{Re}(\text{O})(\text{L}_{\text{O-N}})_2\text{Cl}$  from the Herrmann group<sup>5b</sup> and from the Möscher-Zanetti group<sup>5d</sup> suggest that steric hindrance of  $\text{L}_{\text{O-N}}$  ligands favor the formation of the  $N,N\text{-trans}$  isomer over the  $N,N\text{-cis}$  isomer. However, these trends were deduced from a small number of  $\text{Re}(\text{O})(\text{L}_{\text{O-N}})_2\text{Cl}$  analogues synthesized in individual studies. The majority of  $\text{Re}(\text{O})(\text{L}_{\text{O-N}})_2\text{Cl}$  complexes prepared with similar or larger sized *hoz* analogues, including aryloxides (e.g., phenolates, naphtholates) linked with thiazoline, pyrazoles, and benzoheterocycles (e.g., benzoxazole, benzothiazole, benzimidazole and benzotriazole), were reported as  $N,N\text{-cis}$ .<sup>5e-g</sup> Therefore, *hoz* is a relatively unique

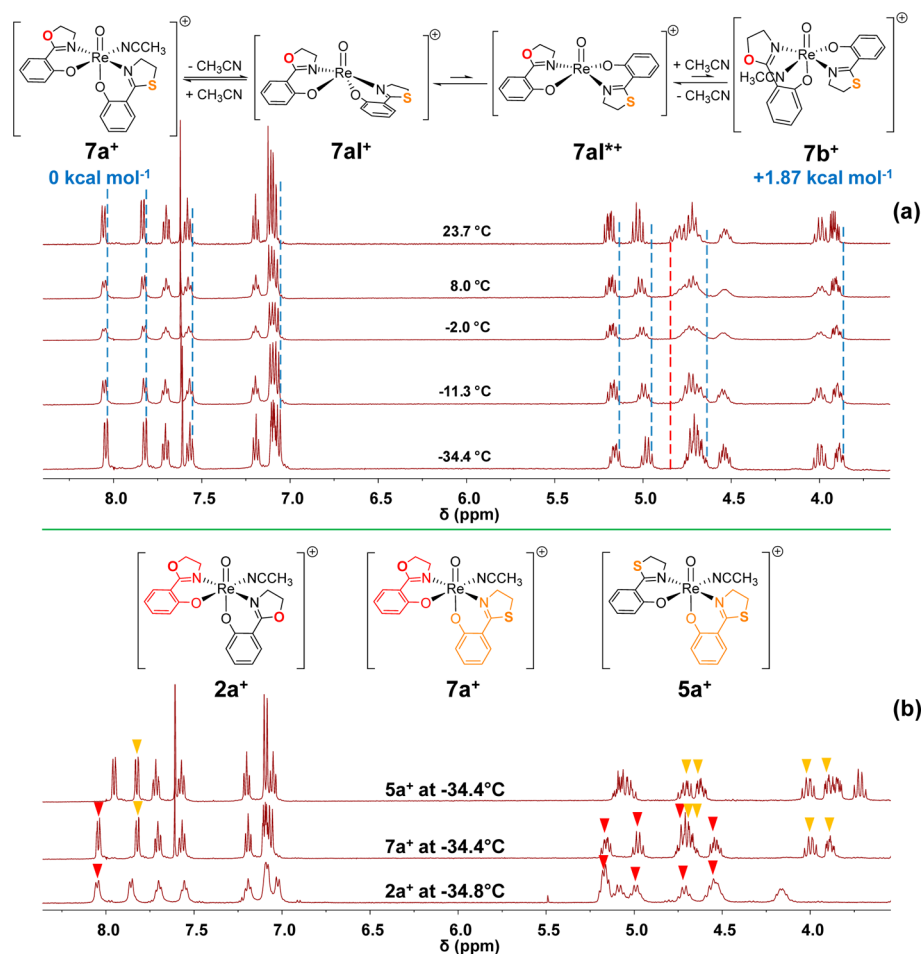


**Figure 9.** (a) VT  $^1H$  NMR (500 MHz,  $CD_3CN$ ) spectra and proposed ligand exchange mechanism for  $7a^+$ . DFT-calculated relative Gibbs free energies for  $7a^+$  and  $7b^+$  (in  $CH_3CN$  at  $25^\circ C$ ) are provided. Dotted lines indicate the shift of resonances from  $23.7^\circ C$  to  $-34.4^\circ C$ . (b) Comparative assignment of  $^1H$  NMR resonances from equatorial *hoz* and axial *htz* ligands in the three  $N,N$ -*trans* cations.

ligand favoring  $N,N$ -*trans* structure. Preparation of the thermodynamically favored  $7a$  as  $N,N$ -*trans* suggests a promising strategy for tuning both structure and functionality via ligand hybridization. In this specific case, *hoz* contributed to the metal economy and ease of synthesis of the desired  $N,N$ -*trans* OS hybrid structure  $7a$  for  $ClO_4^-$  reduction catalysis. As an additional note, attempts at forming  $7a$  by heating a 1:1 mixture of the homoleptic  $N,N$ -*cis* complexes  $2b$  and  $5b$  were unsuccessful. The lack of conversion of the two starting complexes suggests no intermolecular  $L_{O-N}$  ligand exchange.

Kinetically controlled formation of the 1:1 mixture of  $N,N$ -*trans* and  $N,N$ -*cis* isomers at the beginning of synthesis and the thermodynamically controlled isomer interconversion with prolonged heating suggest that opportunities to identify and isolate  $Re(O)(L_{O-N})_2Cl$  isomers might have been missed in earlier reports. In the majority of studies, the reaction mixtures were heated for 2 to 48 h.<sup>21</sup> During these times, different isomers might have converted to the thermodynamically favorable configuration ( $N,N$ -*cis* in majority of cases). Besides, crystallization from a mixture of isomers may have created artifacts in the determination of the targeted compound. This could further lead to incorrect interpretation during the subsequent elucidation of reaction mechanisms and structure–property relationships. For example, the crystal structure of  $Re(O)(hpz)_2Cl$  (*hpz* = 3-(2'-hydroxyphenyl)-1-methyl-1H-pyrazole) was reported as  $N,N$ -*cis*; however, the corresponding

cationic  $[Re(O)(hpz)_2(NCMe)]^+$  formed after chloride abstraction was reported as  $N,N$ -*trans*.<sup>5e</sup> As another example, the crystal structure obtained for  $[Re^{VII}(O)_2(hoz)_2]^+$  following oxidation of  $2a^+$  was reported as  $N,N$ -*cis*;<sup>23b</sup> however, both our experimental observation and the earlier DFT calculations<sup>20</sup> suggest that  $N,N$ -*trans* and  $N,N$ -*cis* structures do not interconvert during  $ClO_4^-$  reduction catalysis. Thus, the most reasonable explanation for these unexpected isomer “conversions” is the presence of an isomeric impurity, which preferentially formed easy-to-distinguish single crystals that were selected by investigators for X-ray analysis. Therefore, for the synthesis of a variety of oxorhenium complexes,  $Me_2Py$ -promoted isomer conversion might serve as a convenient method to minimize or eliminate other isomers in the raw product, thus enabling facile product purification and reducing the possibility of getting incorrect structural and mechanistic information.

**Structure–Activity Relationship and Reaction Mechanisms.** Results in this contribution demonstrate the critical role that the Re coordination sphere plays in catalyst activity. Rates of solvent ligand exchange are 3 orders of magnitude different between two isomers (i.e., 5300-fold for  $2a^+$  versus  $2b^+$ ; 3600-fold for  $5a^+$  versus  $5b^+$ ). From the data in Table 2, the corresponding activation energy differences ( $\Delta\Delta G^\ddagger$ ) at  $25^\circ C$  are  $5.1 \text{ kcal mol}^{-1}$  and  $4.8 \text{ kcal mol}^{-1}$ , respectively. In previous studies,<sup>20,23b</sup> this solvent dissociation was assumed as a

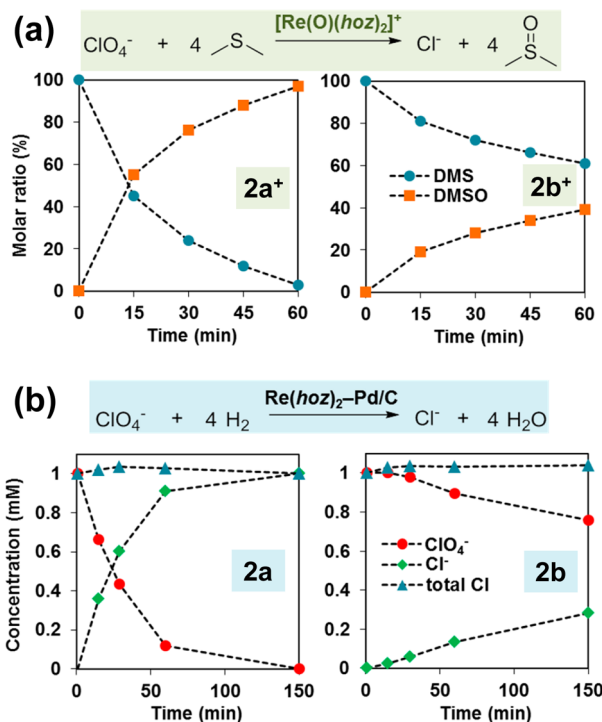
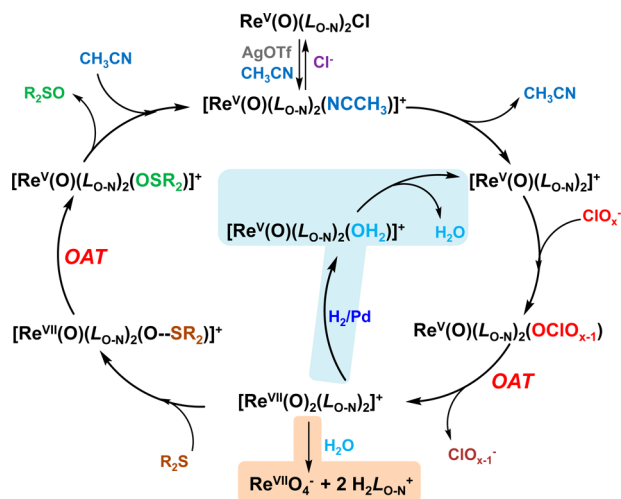


**Figure 10.** (a) Homogeneous  $\text{ClO}_4^-$  reduction (as indicated by sulfide oxidation) catalyzed with  $2a^+$  and  $2b^+$ . Reaction conditions: Re (4 mM),  $\text{LiClO}_4$  (100 mM), and  $\text{Me}_2\text{S}$  (400 mM) in 95/5 (v/v)  $\text{CD}_3\text{CN}/\text{D}_2\text{O}$  at 25 °C. (b) Heterogeneous aqueous  $\text{ClO}_4^-$  reduction by 1 atm  $\text{H}_2$  catalyzed with  $\text{Re}(\text{hoz})_2\text{-Pd/C}$  prepared from  $2a$  and  $2b$ . Reaction conditions: catalyst (5 wt % Re and 5 wt % Pd, 500 mg  $\text{L}^{-1}$ ) and  $\text{NaClO}_4$  (1 mM) in pH 3 water at 25 °C.

### Scheme 1. Proposed Mechanism of Re-Catalyzed $\text{ClO}_4^-$ Reduction<sup>a</sup>



<sup>a</sup>The blue area indicates the heterogeneous catalysis pathway; the orange area indicates the decomposition pathway.

fast step, and the rate-determining step (RDS) was proposed to be the reaction between five-coordinate  $[\text{Re}(\text{O})(\text{hoz})_2]^+$  and  $\text{ClO}_4^-$ . DFT-calculated  $\Delta\Delta G^\ddagger$  on this simplified reaction model was 9.9 kcal  $\text{mol}^{-1}$ .<sup>20</sup> Direct comparison between the DFT-calculated  $\Delta\Delta G^\ddagger$  and measured  $\Delta\Delta G^\ddagger$  for two different steps is not meaningful; however, the values are the same order of magnitude and imply a possible scenario where multiple

**Table 3. Summary of 1 mM Aqueous  $\text{ClO}_4^-$  Reduction Kinetics by Heterogeneous Re–Pd/C Catalysts**

catalyst precursor	pseudo-first-order rate constant ( $\text{L h}^{-1} \text{g}_{\text{cat}}^{-1}$ ) <sup>a</sup>
2a	$5.81 \pm 0.17$
2b	$0.24 \pm 0.02$
5a	$1.03 \pm 0.02$
5b	no reaction
7a	$2.03 \pm 0.04$
$\text{ReO}_4^-$	$0.047 \pm 0.003$

<sup>a</sup>Errors represent 95% confidence intervals.

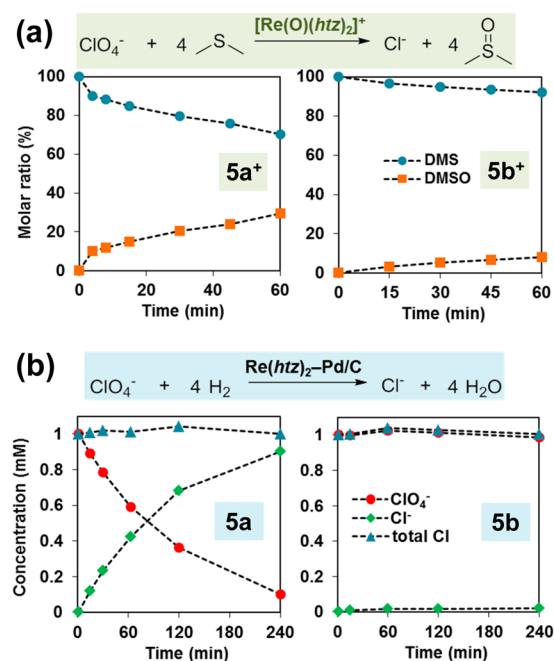


**Figure 11.** (a) Homogeneous  $\text{ClO}_4^-$  reduction catalyzed with  $5a^+$  and  $5b^+$  and (b) heterogeneous  $\text{ClO}_4^-$  reduction catalyzed with  $\text{Re}(\text{htz})_2\text{-Pd/C}$  prepared from  $5a$  and  $5b$ . Reaction conditions are the same as those described in Figure 10.

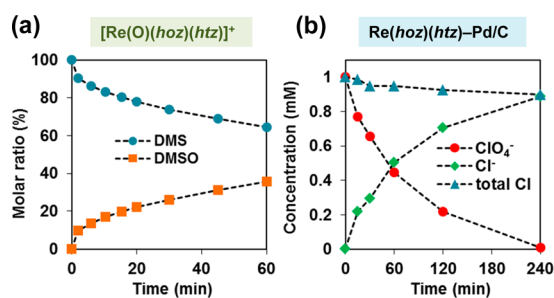


**Figure 12.** (a) Homogeneous  $\text{ClO}_4^-$  reduction catalyzed with  $7a^+$  and (b) heterogeneous  $\text{ClO}_4^-$  reduction catalyzed with  $\text{Re}(\text{hoz})(\text{htz})\text{-Pd/C}$  prepared from  $7a$ . Reaction conditions are the same as those described in Figure 10.

steps (Scheme 1) determine the overall reaction rate. Also, we observed markedly different rates of sulfide dissociation (i.e., much slower from  $2b^+$  than from  $2a^+$ ) and chloride dissociation (i.e.,  $5b$  requires a high temperature to react with  $\text{AgOTf}$ ) from these isomers. Re–Cl bond distances in *N,N-cis* structures are generally shorter than those in *N,N-trans* structures (Table S2), but a quantitative correlation for the five complexes was not observed between Re–Cl distances and ligand dissociation

kinetics. A deeper mechanistic understanding in future efforts might necessitate examination of energy levels and electronic structures of transition states and intermediates involved in multiple reaction steps, as well as an upgraded reaction model for the overall catalytic cycle.

Heterogenization in the activated carbon matrix facilitated activity evaluation of individual Re complexes. During homogeneous  $\text{ClO}_4^-$  reduction (TON = 100 upon completion) using presynthesized *N,N-trans*  $[\text{Re}(\text{O})(\text{L}_{\text{O-N}})_2]^+$ , the dominant Re species in solution after the reaction started was  $\text{Re}(\text{O})(\text{L}_{\text{O-N}})_2\text{Cl}$ . Except for **2a**, all Re complexes were severely inhibited by the  $\text{Cl}^-$  product before 50%  $\text{ClO}_4^-$  was reduced. In contrast, during the immobilization of  $\text{Re}(\text{O})(\text{L}_{\text{O-N}})_2\text{Cl}$  precursors in Pd/C, 0.134 mM Re-bound  $\text{Cl}^-$  was quantitatively released in water that already contained 1 mM HCl. For all **OO-**, **SS-**, and **OS-Pd/C** catalysts, pseudo-first-order kinetics were consistent during the complete reduction of 1–4 mM  $\text{ClO}_4^-$  (TON = 30–120). It appears that immobilized Re species on carbon surface have substantially lowered affinity with aqueous  $\text{Cl}^-$ . Except for  $\text{H}_2\text{O}$  (and  $\text{OH}^-$ ), the aqueous phase does not contain other ligands, such as acetonitrile, sulfide, and sulfoxide involved in homogeneous catalysis. Therefore, as reflected by heterogeneous  $\text{ClO}_4^-$  reduction kinetics (Table 3), the intrinsic activity order for the five complexes is **2a** > **7a** > **5a** > **2b** > **5b**. The ligand effect on the overall catalytic activity with the same *N,N-trans* or *N,N-cis* coordination sphere is thus **OO** > **OS** > **SS**.

**Significance in Water Technology Innovation.** Perchlorate contamination of drinking water supplies is a serious problem that recently caused several incidents of water supply interruption in California.<sup>29</sup> A life cycle assessment (LCA) study<sup>30</sup> for drinking water treatment of  $\text{ClO}_4^-$  indicated that >20-fold activity improvement of the first generation bimetallic  $\text{ReO}_x\text{-Pd/C}$  catalyst (prepared from reductive immobilization of  $\text{ReO}_4^-$ )<sup>31</sup> is necessary for catalytic treatment to be competitive with conventional water treatment technologies (ion exchange and biological reduction). Therefore, improving reactivity of the immobilized Re component is vital for reducing the loadings of immobilized Re and Pd. The activities of  $\text{Re}(\text{O})(\text{L}_{\text{O-N}})_2\text{-Pd/C}$  catalyst prepared from **2a**, **5a**, and **7a** are approximately 110, 20, and 40 times more active than  $\text{ReO}_x\text{-Pd/C}$ . In contrast, the catalyst prepared from **2b** is merely 4 times more active than  $\text{ReO}_x\text{-Pd/C}$ , and the one prepared from **5b** shows no activity. Therefore, developing effective strategies for isomer control contributes both fundamental understanding of oxorhenium chemistry and supports the development of innovative and practical water treatment technologies. Further ligand structure modification is feasible to continue the fine-tuning of Re complex reactivity, provided that these ligands favor the formation of desired isomeric structures. The successful immobilization of five different complexes in Pd/C matrix also demonstrates that the organometallic Re complex module in the biomimetic catalyst can be flexibly replaced with a wider selection of structures.

**Implications in Ligand Exchange Dynamics.** Findings in this study highlight a collection of strategies for controlling ligand exchange dynamics. As summarized in Table 2, coarse adjustment (i.e., orders of magnitude range) can be realized by coordination sphere design, and fine-tuning (i.e., 3–5 times) can be realized by ligand structure design. As suggested by VT NMR observation, complexes with homoleptic and heteroleptic ligand coordination exhibited different ligand movement patterns, which impact the molecular shape that is important

for biomedical design.<sup>3c,e</sup> Thus, rationally tuned ligand exchange kinetics and patterns might influence the activity and stability of functional oxorhenium complexes in both catalysis and biomedical applications. The fundamental coordination chemistry acquired from oxorhenium might also be transferred to develop oxomolybdenum<sup>32</sup> and oxotungsten<sup>33</sup> complexes. Tunable functionalities of these complexes are anticipated to inspire innovation in a broad range of environmental, energy, and healthcare technologies.

## CONCLUSIONS

Three *N,N-trans*  $\text{Re}(\text{O})(\text{L}_{\text{O-N}})_2\text{Cl}$  complexes (**2a**, **5a**, and **7a**) and two *N,N-cis*  $\text{Re}(\text{O})(\text{L}_{\text{O-N}})_2\text{Cl}$  complexes (**2b** and **5b**) were synthesized. For **OO** and **SS** complexes, a 1:1 mixture of *N,N-trans* and *N,N-cis* isomers were initially obtained, and the mixtures fully converted to thermodynamically favored **2a** and **5b** upon heating in ethanol with excess  $\text{Me}_2\text{Py}$  base. The hybrid **OS** complex synthesized with two opposite  $\text{L}_{\text{O-N}}$  addition sequences afforded the same product **7a** as *N,N-trans*  $\text{Re}(\text{O})(\text{hoz})_{\text{eq}}(\text{htz})_{\text{ax}}\text{Cl}$ . Cationic *N,N-trans* complexes exhibited 3 orders of magnitude faster solvent ligand dissociation and intramolecular  $\text{L}_{\text{O-N}}$  exchange than the corresponding *N,N-cis* isomers. With the same Re coordination sphere, *htz* resulted in a slower ligand exchange than *hoz*. The *ax/eq* preference of *htz* and *hoz* in the hybrid **7a**<sup>+</sup> reduced  $\text{L}_{\text{O-N}}$  movement and  $\Delta S^\ddagger$  for solvent dissociation, thus leading to a slower ligand exchange than both **2a**<sup>+</sup> and **5a**<sup>+</sup>. The order of ligand exchange rates of the five complexes roughly correlated with the order of overall  $\text{ClO}_4^-$  reduction rates at the heterogeneous  $\text{Re}(\text{L}_{\text{O-N}})_2\text{-Pd/C}$  catalyst surface. Selective synthesis of *N,N-trans* structures significantly contribute to the application of catalytic  $\text{ClO}_4^-$  treatment in water. The mechanistic insights benefit the development of functional coordination complexes of Re and other metals for a wide range of applications.

## EXPERIMENTAL SECTION

**General information.** All chemicals and solvents were purchased from Alfa-Aesar, Sigma-Aldrich, and Cambridge Isotope Laboratories, and used as received. NMR (Varian Unity INOVA, operating at a spectral frequency of 499.432 MHz), X-ray structure determination, and elemental analysis were conducted in the NMR Laboratory, George L. Clark X-ray Facility and 3M Materials Laboratory, and the Microanalysis Laboratory in the University of Illinois School of Chemical Sciences, respectively. Temperatures for VT-NMR were calibrated with methanol (<25 °C) and ethylene glycol (>25 °C). Half-height line width values were determined automatically using Vnmr 6.1c. Aqueous solutions were prepared using deionized (DI) water (Barnstead Nanopure system; resistivity >17.5 MΩ cm). UV-vis measurements were conducted on a Shimadzu 2550 spectrophotometer with solvent as background. Unless specified, all procedures were conducted under air.

**Preparation of 2-(2'-hydroxyphenyl)-2-oxazoline (Hhoz).** A mixture of 2-hydroxybenzoinitrile (1.19 g, 10 mmol), ethanolamine (0.73 g, 12 mmol),  $\text{ZnCl}_2$  (68 mg, 0.5 mmol), and toluene (10 mL) was refluxed in a 25 mL flask for 24 h. Then, the solvent was removed *in vacuo*, and the residue was extracted with five portions of 5 mL of  $\text{Et}_2\text{O}$ . The combined organic phase was dried, and the residue was dissolved in EtOAc and purified by silica gel flash chromatography (hexanes/EtOAc = 4/1) to provide the product as a colorless oil, which turned into a slightly orange-pink solid after being placed at –20 °C overnight. Yield: 1.20 g (74%). Characterization data matched those in the previous report.<sup>34</sup>

**Preparation of *N,N-trans*  $\text{Re}(\text{O})(\text{hoz})_2\text{Cl}$  (**2a**).** A mixture of  $\text{Re}(\text{O})(\text{OPPh}_3)(\text{SMMe}_2)\text{Cl}_3$  (500 mg, 0.770 mmol), *Hhoz* (277 mg, 1.70

mmol), 2,6-lutidine (490  $\mu$ L, 454 mg, 4.24 mmol), and EtOH (30 mL) was refluxed in a 50 mL flask. The mixture turned gray-brown in the first 5 min and then gradually turned forest green over the following 10 min. The green suspension was refluxed for 48 h. After cooling down and filtering off the liquid phase through a glass frit, the solid phase was sequentially washed with  $3 \times 2$  mL of EtOH and  $3 \times 1$  mL of Et<sub>2</sub>O to afford a green powder. Yield: 383 mg (88%). <sup>1</sup>H NMR (500 MHz, CDCl<sub>3</sub>)  $\delta$  7.90 (dd,  $J = 8.1, 1.8$  Hz, 1H), 7.66 (dd,  $J = 7.9, 1.8$  Hz, 1H), 7.41 (ddd,  $J = 8.7, 7.0, 1.8$  Hz, 1H), 7.20 (ddd,  $J = 8.6, 7.3, 1.8$  Hz, 1H), 6.93 (ddd,  $J = 8.2, 7.2, 1.1$  Hz, 1H), 6.85 (dd,  $J = 8.6, 1.2$  Hz, 1H), 6.80–6.75 (m, 2H), 5.09–4.74 (m, 6H), 4.32–4.21 (m, 2H). Elemental analysis (C<sub>18</sub>H<sub>16</sub>N<sub>2</sub>O<sub>3</sub>ClRe) calculated: C, 38.47%; H, 2.87%; N, 4.98%; Cl, 6.31%; Re, 33.13%. Found: C, 38.34%; H, 2.56%; N, 4.90%; Cl, 6.14%; Re, 32.10%. UV–vis spectra in CH<sub>2</sub>Cl<sub>2</sub> solution are shown in Figure S9a and b. Single crystals suitable for X-ray diffraction were grown by diffusion of pentane into the CH<sub>2</sub>Cl<sub>2</sub> solution of the product.

**Preparation of *N,N*-cis Re(O)(hoz)<sub>2</sub>Cl (2b).** A mixture of Re(O) (OPPh<sub>3</sub>)(SMe<sub>2</sub>)Cl<sub>3</sub> (100 mg, 0.154 mmol), Hhoz (55 mg, 0.337 mmol), 2,6-di-*tert*-butylpyridine (84  $\mu$ L, 72 mg, 0.374 mmol), and EtOH (6 mL) was refluxed in a 10 mL flask for 15 min. The mixture turned forest green in the first 5 min. After cooling down and filtering, the solid phase was washed with  $2 \times 1$  mL of EtOH and dissolved in CH<sub>2</sub>Cl<sub>2</sub> for silica gel flash chromatography (EtOAc). The product (*R<sub>f</sub>* 0.7) was isolated from the *N,N*-*trans* isomer (tailed) as a green powder after solvent removal *in vacuo*. Yield: 41 mg (47%). <sup>1</sup>H NMR (500 MHz, CDCl<sub>3</sub>)  $\delta$  7.81 (dd,  $J = 8.1, 1.8$  Hz, H), 7.56–7.60 (m, 2H), 7.46 (dd,  $J = 8.6, 1.1$  Hz, 1H), 7.19 (ddd,  $J = 8.6, 7.2, 1.8$  Hz, 1H), 6.94 (ddd,  $J = 8.0, 7.3, 1.0$  Hz, 1H), 6.88 (ddd,  $J = 8.1, 7.1, 1.1$  Hz, 1H), 6.73 (dd,  $J = 8.4, 1.1$  Hz, 1H), 5.01 (ddd,  $J = 10.9, 8.6, 7.7$  Hz, 1H), 4.87 (ddd,  $J = 10.5, 9.5, 8.6$  Hz, 1H), 4.63 (dt,  $J = 10.6, 8.7$  Hz, 1H), 4.52 (dt,  $J = 10.6, 8.5$  Hz, 1H), 4.43 (ddd,  $J = 13.6, 10.8, 9.6$  Hz, 1H), 4.13 (ddd,  $J = 13.6, 10.4, 7.8$  Hz, 1H), 4.01 (ddd,  $J = 12.3, 10.6, 8.4$  Hz, 1H), 3.71 (ddd,  $J = 12.3, 10.6, 8.6$  Hz, 1H). Elemental analysis (C<sub>18</sub>H<sub>16</sub>N<sub>2</sub>O<sub>3</sub>ClRe) calculated: C, 38.47%; H, 2.87%; N, 4.98%; Cl, 6.31%; Re, 33.13%. Found: C, 38.41%; H, 2.71%; N, 4.82%; Cl, 6.37%; Re, 35.70%. UV–vis spectra in CH<sub>2</sub>Cl<sub>2</sub> solution are shown in Figure S9a and b. Single crystals suitable for X-ray diffraction were grown by diffusion of toluene into the CH<sub>2</sub>Cl<sub>2</sub> solution of the product.

**Preparation of [H<sub>2</sub>hoz][Re(O)(hoz)Cl<sub>3</sub>] (3).** A mixture of Re(O) (OPPh<sub>3</sub>)(SMe<sub>2</sub>)Cl<sub>3</sub> (81 mg, 0.125 mmol), Hhoz (43 mg, 0.264 mmol), and EtOH (5 mL) was refluxed in a 10 mL flask for 15 min. After solvent removal *in vacuo*, the addition of chloroform (2 mL) converted the residual green oil into a solid phase. The liquid phase was then filtered off to afford a light green powder. Yield: 30 mg (38%). <sup>1</sup>H NMR (500 MHz, CD<sub>3</sub>CN)  $\delta$  10.17 (br, 2H), 7.90 (dd,  $J = 8.1, 1.7$  Hz, 1H), 7.74 (ddd,  $J = 8.9, 7.3, 1.7$  Hz, 1H), 7.60 (dd,  $J = 7.9, 1.8$  Hz, 1H), 7.29 (d,  $J = 8.4$  Hz, 1H), 7.23 (ddd,  $J = 8.8, 7.3, 1.8$  Hz, 1H), 7.16 (ddd,  $J = 8.1, 7.4, 1.0$  Hz, 1H), 7.00 (ddd,  $J = 7.9, 7.2, 0.8$  Hz, 1H), 6.80 (d,  $J = 8.3$  Hz, 1H), 5.03 (t,  $J = 9.8$  Hz, 2H), 4.92 (t,  $J = 9.6$  Hz, 2H), 4.22 (t,  $J = 9.8$  Hz, 2H), 3.83 (t,  $J = 9.6$  Hz, 2H). Elemental analysis (C<sub>18</sub>H<sub>18</sub>N<sub>2</sub>O<sub>3</sub>Cl<sub>3</sub>Re) calculated: C, 34.05%; H, 2.86%; N, 4.41%; Cl, 16.75%; Re, 29.30%. Found: C, 33.72%; H, 2.65%; N, 4.28%; Cl, 15.11%; Re, 30.03%. Single crystals suitable for X-ray diffraction were grown from the chloroform of the product.

**Preparation of [H-*t*Bu<sub>2</sub>Py][Re(O)(hoz)Cl<sub>3</sub>] (4).** In a 25 mL flask, Re(O) (OPPh<sub>3</sub>)(SMe<sub>2</sub>)Cl<sub>3</sub> (300 mg, 0.462 mmol) was stirred in 10 mL of boiling ethanol as a pale green suspension. Hhoz (76 mg, 0.467 mmol) dissolved in 2 mL of ethanol was slowly added into the flask over 45 min via a 1 mL syringe. The solution gradually turned bright green. Then, 2,6-di-*tert*-butylpyridine (114  $\mu$ L, 97 mg, 0.509 mmol) in 1 mL of ethanol was slowly added in the same way. After heating for another 15 min, the solvent was removed *in vacuo*. The solid residue was washed with  $3 \times 1$  mL ethanol and  $3 \times 1$  mL diethyl ether to afford a light green powder. Yield: 233 mg (76%). <sup>1</sup>H NMR (500 MHz, CD<sub>3</sub>CN)  $\delta$  11.21 (br, 1H), 8.47 (t,  $J = 8.2$  Hz, 1H), 7.91 (d,  $J = 8.2$  Hz, 2H), 7.60 (dd,  $J = 7.9, 1.8$  Hz, 1H), 7.23 (ddd,  $J = 8.4, 7.3, 1.8$  Hz, 1H), 7.00 (ddd,  $J = 8.1, 7.2, 1.1$  Hz, 1H), 6.80 (dd,  $J = 8.3, 1.1$  Hz, 1H), 4.92 (t,  $J = 9.6$  Hz, 2H), 3.83 (t,  $J = 9.6$  Hz, 2H), 1.54 (s, 18H). The resonances corresponding to the Re-coordinated hoz match those

in [H<sub>2</sub>hoz][Re(O)(hoz)Cl<sub>3</sub>]. Elemental analysis (C<sub>22</sub>H<sub>30</sub>N<sub>2</sub>O<sub>3</sub>Cl<sub>3</sub>Re) calculated: C, 39.85%; H, 4.56%; N, 4.22%; Cl, 16.04%; Re, 28.08%. Found: C, 39.32%; H, 4.32%; N, 4.16%; Cl, 13.89%; Re, 28.34%.

**Preparation of 2-(2'-hydroxyphenyl)-2-thiazole (Hhtz).** A mixture of 2-hydroxybenzotrile (1.19 g, 10 mmol), cysteamine (0.85 g, 11 mmol), ZnCl<sub>2</sub> (27 mg, 0.2 mmol), and MeOH (10 mL) was refluxed in a 25 mL flask under N<sub>2</sub> for 5 h. Then, the solvent was removed *in vacuo*, and the residue was extracted with five portions of 5 mL of diethyl ether. The combined organic phase was dried, and the residue was dissolved in EtOAc and purified by silica gel flash chromatography (hexanes/EtOAc = 4/1) to provide the product as a yellow oil, which turned into a yellow solid after being placed at –20 °C overnight. Yield: 1.53 g (85%). Characterization data matched those in previous reports.<sup>5a</sup>

**Preparation of *N,N*-trans Re(O)(htz)<sub>2</sub>Cl (5a).** A mixture of Re(O) (OPPh<sub>3</sub>)(SMe<sub>2</sub>)Cl<sub>3</sub> (200 mg, 0.308 mmol), Hhtz (116 mg, 0.647 mmol), 2,6-di-*tert*-butylpyridine (160  $\mu$ L, 136 mg, 0.712 mmol), and EtOH (18 mL) was refluxed in a 25 mL flask for 15 min. The product was filtered and washed with  $2 \times 2$  mL of EtOH and  $2 \times 1$  mL of Et<sub>2</sub>O as an ~1:1 mixture of *N,N*-*trans* and *N,N*-*cis* isomers. The mixture was collected in a 20 mL vial and extracted with 3 times of 5 mL of CHCl<sub>3</sub>. Each extraction used sonication for 15 s and occasional shaking during the following 30 min. Clarified CHCl<sub>3</sub> solution was combined and dried. The green solid residue rich in the *N,N*-*trans* isomer was further purified by three rounds of recrystallization with CH<sub>2</sub>Cl<sub>2</sub>/pentane followed by quick CHCl<sub>3</sub> extraction. Yield: 84 mg (46%). <sup>1</sup>H NMR (500 MHz, CDCl<sub>3</sub>)  $\delta$  7.68 (dd,  $J = 8.1, 1.6$  Hz, 1H), 7.55 (dd,  $J = 7.9, 1.6$  Hz, 1H), 7.38 (ddd,  $J = 8.6, 7.1, 1.6$  Hz, 1H), 7.17 (ddd,  $J = 8.5, 7.3, 1.6$  Hz, 1H), 6.95 (ddd,  $J = 8.1, 7.3, 1.1$  Hz, 1H), 6.78 (dd,  $J = 8.3, 0.9$  Hz, 1H), 6.75–6.70 (m, 2H), 5.53 (ddd,  $J = 14.8, 9.1, 5.7$  Hz, 1H), 5.09 (ddd,  $J = 14.8, 10.4, 9.2$  Hz, 1H), 4.59 (ddd,  $J = 14.5, 9.2, 5.4$  Hz, 1H), 4.41 (ddd,  $J = 14.5, 10.4, 9.1$  Hz, 1H), 3.86 (td,  $J = 10.6, 9.3$  Hz, 1H), 3.71 (m, 2H), 3.60 (td,  $J = 10.6, 9.2$  Hz, 1H). Elemental analysis (C<sub>18</sub>H<sub>16</sub>N<sub>2</sub>O<sub>3</sub>S<sub>2</sub>ClRe) calculated: C, 36.39%; H, 2.71%; N, 4.72%; S, 10.79%; Cl, 5.97%; Re, 31.34%. Found: C, 36.28%; H, 2.68%; N, 4.63%; S, 10.67%; Cl, 5.70%; Re, 30.95%. UV–vis spectra in CH<sub>2</sub>Cl<sub>2</sub> solution are shown in Figure S9c and d. Single crystals suitable for X-ray diffraction were grown by diffusion of toluene into the CH<sub>2</sub>Cl<sub>2</sub> solution of the product.

**Preparation of *N,N*-cis Re(O)(htz)<sub>2</sub>Cl (5b).** A mixture of Re(O) (OPPh<sub>3</sub>)(SMe<sub>2</sub>)Cl<sub>3</sub> (167 mg, 0.257 mmol), Hhtz (102 mg, 0.566 mmol), 2,6-lutidine (164  $\mu$ L, 151 mg, 1.407 mmol), and EtOH (10 mL) was refluxed in a 25 mL flask for 48 h. The product was filtered and washed with  $3 \times 2$  mL of EtOH and  $3 \times 1$  mL of Et<sub>2</sub>O to afford a green powder. Yield: 140 mg (92%). <sup>1</sup>H NMR (500 MHz, CDCl<sub>3</sub>)  $\delta$  7.56 (ddd,  $J = 8.6, 7.0, 1.7$  Hz, 1H), 7.52 (dd,  $J = 8.0, 1.7$  Hz, 1H), 7.46–7.43 (m, 2H), 7.16 (ddd,  $J = 8.6, 7.2, 1.7$  Hz, 1H), 6.94 (ddd,  $J = 8.2, 7.3, 1.2$  Hz, 1H), 6.82 (ddd,  $J = 8.1, 7.0, 1.2$  Hz, 1H), 6.51 (dd,  $J = 8.4, 1.1$  Hz, 1H), 4.73 (dt,  $J = 14.9, 9.9$  Hz, 1H), 4.61 (ddd,  $J = 14.7, 8.0, 6.4$  Hz, 1H), 4.11 (ddd,  $J = 13.8, 11.5, 8.3$  Hz, 1H), 3.89 (ddd,  $J = 13.5, 8.5, 4.6$  Hz, 1H), 3.87–3.79 (m, 2H), 3.19 (ddd,  $J = 10.9, 8.4, 4.5$  Hz, 1H), 2.51 (td,  $J = 11.2, 8.5$  Hz, 1H). Elemental analysis (C<sub>18</sub>H<sub>16</sub>N<sub>2</sub>O<sub>3</sub>S<sub>2</sub>ClRe) calculated: C, 36.39%; H, 2.71%; N, 4.72%; S, 10.79%; Cl, 5.97%; Re, 31.34%. Found: C, 35.68%; H, 2.67%; N, 4.56%; S, 10.50%; Cl, 5.32%; Re, 30.83%. UV–vis spectra in CH<sub>2</sub>Cl<sub>2</sub> solution are shown in Figure S9c and d. Single crystals suitable for X-ray diffraction were grown by diffusion of pentane into the CH<sub>2</sub>Cl<sub>2</sub> solution of the product.

**Preparation of [H-*t*Bu<sub>2</sub>Py][Re(O)(htz)Cl<sub>3</sub>] (6).** Hhtz (42 mg, 0.233 mmol) dissolved in 1 mL of ethanol was slowly added, via a 1 mL syringe over 15 min, into the 15 mL flask with Re(O) (OPPh<sub>3</sub>)(SMe<sub>2</sub>)Cl<sub>3</sub> (150 mg, 0.231 mmol) suspension in 5 mL of boiling ethanol. The solution gradually turned dark green. Then, 2,6-di-*tert*-butylpyridine (57  $\mu$ L, 49 mg, 0.254 mmol) in 1 mL of ethanol was slowly added in the same way. Deep green powders precipitated out when about a half of 2,6-di-*tert*-butylpyridine was added. After cooling down and filtration, the solid was washed with  $3 \times 1$  mL of ethanol and  $3 \times 1$  mL of diethyl ether to afford a deep green powder. Yield: 122 mg (78%). <sup>1</sup>H NMR (500 MHz, CD<sub>3</sub>CN)  $\delta$  11.18 (br, 1H), 8.46 (br, 1H), 7.90 (br, 2H), 7.50 (dd,  $J = 7.9, 1.7$  Hz, 1H), 7.20 (ddd,  $J =$

8.7, 7.2, 1.7 Hz, 1H), 7.02 (ddd,  $J = 8.2, 7.2, 1.2$  Hz, 1H), 6.82 (dd,  $J = 8.3, 1.2$  Hz, 1H), 4.18 (t,  $J = 8.5$  Hz, 2H), 3.75 (t,  $J = 8.5$  Hz, 2H), 1.54 (s, 18H). Elemental analysis ( $C_{22}H_{30}N_2O_2S_2Cl_3Re$ ) calculated: C, 38.91%; H, 4.45%; N, 4.12%; Cl, 15.66%; Re, 27.42%; S, 4.72%. Found: C, 38.06%; H, 4.20%; N, 4.08%; Cl, 14.43%; Re, 28.35%; S, 5.14%. Single crystals suitable for X-ray diffraction were grown by diffusion of pentane into the  $CH_2Cl_2$  solution of the product.

**Preparation of *N,N*-trans  $Re(O)(hoz)_{eq}(htz)_{ax}Cl$  (7a).** A mixture of [H-di-*t*Bu-Py][ $Re(O)(hoz)Cl_3$ ] (230 mg, 0.347 mmol), Hhtz (63 mg, 0.353 mmol), 2,6-lutidine (42  $\mu$ L, 39 mg, 0.364 mmol), and EtOH (15 mL) was refluxed in a 25 mL flask for 15 min. Then, another portion of excess 2,6-lutidine (121  $\mu$ L, 112 mg, 1.05 mmol) was added, and the mixture was kept under reflux for 48 h. The product was filtered and washed with  $3 \times 2$  mL of EtOH and  $3 \times 1$  mL of Et<sub>2</sub>O to afford a green powder. Yield: 163 mg (81%). Further purification was conducted by slow crystallization from saturated  $CHCl_3$  solution. <sup>1</sup>H NMR (500 MHz,  $CDCl_3$ )  $\delta$  7.92 (dd,  $J = 8.1, 1.8$  Hz, 1H), 7.57 (dd,  $J = 7.9, 1.6$  Hz, 1H), 7.43 (ddd,  $J = 8.6, 7.0, 1.8$  Hz, 1H), 7.20 (ddd,  $J = 8.3, 7.2, 1.6$  Hz, 1H), 6.96 (t,  $J = 7.6$  Hz, 1H), 6.84 (d,  $J = 8.5$  Hz, 1H), 6.82–6.78 (m, 2H), 5.10–5.04 (m, 1H), 4.93–4.78 (m, 3H), 4.69 (ddd,  $J = 14.4, 9.1, 5.3$  Hz, 1H), 4.51 (dt,  $J = 14.4, 9.8$  Hz, 1H), 3.87 (q,  $J = 10.6, 9.1$  Hz, 1H), 3.74 (ddd,  $J = 10.9, 9.0, 5.3$  Hz, 1H). Elemental analysis ( $C_{18}H_{16}N_2O_2S_2ClRe$ ) calculated: C, 37.40%; H, 2.79%; N, 4.85%; Cl, 6.13%; Re, 32.21%; S, 5.55%. Found: C, 36.63%; H, 2.65%; N, 4.70%; Cl, 6.67%; Re, 32.32%; S, 4.97%. UV–vis spectra in  $CH_2Cl_2$  solution are shown in Figure S9e and f. Single crystals suitable for X-ray diffraction were grown by diffusion of pentane into the  $CH_2Cl_2$  solution of the product.

**Preparation of  $[Re(O)(L)_2][OTf]$  in  $CD_3CN$ .** In general,  $Re(O)(L)_2Cl$  reacted with 1.05 equiv of  $AgOTf$  in  $CD_3CN$  (1 mL for every 10 mg of Re complex) at room temperature for 30 min. For *N,N*-*cis*  $Re(O)(htz)_2Cl$ , reflux for 2 h was necessary. The white  $AgCl$  precipitate was filtered off through a glass pipet filled with glass wool. The resulting dark green solutions were stored at  $-20$  °C until characterization and homogeneous  $ClO_4^-$  reduction catalysis. UV–vis spectra in  $CH_3CN$  solution are shown in Figure S10.

***N,N*-trans  $[Re(O)(hoz)_2]^+$  (2a<sup>+</sup>).** <sup>1</sup>H NMR (500 MHz,  $CD_3CN$ )  $\delta$  7.97 (d,  $J = 7.8$  Hz, 2H), 7.62 (t,  $J = 7.7$  Hz, 2H), 7.14 (t,  $J = 7.7$  Hz, 2H), 7.06 (d,  $J = 8.5$  Hz, 2H), 5.18 (ddd,  $J = 10.9, 8.6, 7.0$  Hz, 2H), 5.06 (dt,  $J = 10.3, 8.7$  Hz, 2H), 4.71–4.59 (m, 2H), 4.37 (br, 2H) (at room temperature).

***N,N*-*cis*  $[Re(O)(hoz)_2]^+$  (2b<sup>+</sup>).** <sup>1</sup>H NMR (500 MHz,  $CD_3CN$ )  $\delta$  7.99 (dd,  $J = 8.1, 1.8$  Hz, 1H), 7.85 (dd,  $J = 7.9, 1.8$  Hz, 1H), 7.74 (ddd,  $J = 8.7, 7.1, 1.8$  Hz, 1H), 7.47 (ddd,  $J = 8.5, 7.3, 1.8$  Hz, 1H), 7.23 (m, 2H), 7.07 (ddd,  $J = 8.1, 7.1, 1.2$  Hz, 1H), 6.90 (dd,  $J = 8.4, 1.1$  Hz, 1H), 5.06 (ddd,  $J = 10.7, 8.7, 7.8$  Hz, 1H), 4.98 (ddd,  $J = 10.5, 9.5, 8.6$  Hz, 1H), 4.82 (dd,  $J = 10.2, 9.0$  Hz, 2H), 4.36 (ddd,  $J = 13.3, 10.8, 9.4$  Hz, 1H), 4.23 (ddd,  $J = 13.4, 10.5, 7.9$  Hz, 1H), 4.12 (dt,  $J = 12.0, 9.3$  Hz, 1H), 3.95 (dt,  $J = 12.1, 9.7$  Hz, 1H) (at room temperature).

***N,N*-trans  $[Re(O)(htz)_2]^+$  (5a<sup>+</sup>).** <sup>1</sup>H NMR (500 MHz,  $CD_3CN$ )  $\delta$  7.89 (d,  $J = 7.8$  Hz, 2H), 7.65 (t,  $J = 7.2$  Hz, 2H), 7.14 (d,  $J = 7.0$  Hz, 2H), 7.11 (dd,  $J = 8.4, 0.9$  Hz, 2H), 4.91 (br, 4H), 3.90 (t,  $J = 8.6$  Hz, 4H) (at room temperature).

***N,N*-*cis*  $[Re(O)(htz)_2]^+$  (5b<sup>+</sup>).** <sup>1</sup>H NMR (500 MHz,  $CD_3CN$ )  $\delta$  7.84 (dd,  $J = 8.1, 1.5$  Hz, 1H), 7.77 (dd,  $J = 8.0, 1.4$  Hz, 1H), 7.74 (ddd,  $J = 8.5, 7.3, 1.6$  Hz, 1H), 7.46 (ddd,  $J = 8.4, 7.4, 1.5$  Hz, 1H), 7.25 (ddd,  $J = 8.2, 7.6, 0.9$  Hz, 1H), 7.21 (dd,  $J = 8.4, 0.9$  Hz, 1H), 7.01 (ddd,  $J = 8.2, 7.2, 1.0$  Hz, 1H), 6.84 (dd,  $J = 8.4, 0.9$  Hz, 1H), 4.78 (ddd,  $J = 14.9, 7.8, 6.9$  Hz, 1H), 4.63 (dt,  $J = 14.9, 9.7$  Hz, 1H), 4.40 (ddd,  $J = 13.9, 9.3, 7.4$  Hz, 1H), 4.11 (dt,  $J = 13.8, 9.2$  Hz, 1H), 3.88–3.85 (m, 1H), 3.57 (q,  $J = 7.2$  Hz, 1H), 3.52 (dt,  $J = 11.2, 9.0$  Hz, 1H), 3.34 (ddd,  $J = 11.2, 9.3, 7.4$  Hz, 1H) (at room temperature).

***N,N*-trans  $[Re(O)(hoz)(htz)]^+$  (7a<sup>+</sup>).** <sup>1</sup>H NMR (500 MHz,  $CD_3CN$ )  $\delta$  8.06 (dd,  $J = 8.3, 1.6$  Hz, 1H), 7.84 (dd,  $J = 8.0, 1.5$  Hz, 1H), 7.70 (ddd,  $J = 8.7, 7.4, 1.7$  Hz, 1H), 7.58 (ddd,  $J = 8.7, 7.3, 1.5$  Hz, 1H), 7.23–7.17 (m, 1H), 7.14–7.07 (m, 3H), 5.19 (ddd,  $J = 10.9, 8.6, 7.1$  Hz, 1H), 5.03 (td,  $J = 10.2, 8.8$  Hz, 1H), 4.81 (ddd,  $J = 14.2, 11.6, 9.5$  Hz, 1H), 4.77–4.68 (m, 2H), 4.53 (td,  $J = 11.1, 7.4$  Hz, 1H), 4.00 (td,  $J = 11.3, 9.3$  Hz, 1H), 3.91 (ddd,  $J = 11.1, 9.2, 4.3$  Hz, 1H) (at room temperature).

**X-ray Crystallography.** Single crystal X-ray diffraction data were collected on different instruments summarized in Table S1. Combinations of  $0.5^\circ \varphi$  and  $\omega$  scans were used to collect the data. The collections, cell refinements, and integrations of intensity data were carried out with the APEX2 software package.<sup>35</sup> Face-indexed absorption corrections were performed numerically with the program XPREP.<sup>36</sup> SADABS<sup>37</sup> was used to make incident beam and decay corrections. The structures were solved with the direct methods program<sup>38</sup> and refined with the full-matrix least-squares SHELXL<sup>39</sup> program. Additional refinement details and metrical parameters are provided in Table S1.

**Computational Details.** DFT<sup>40</sup> was applied to structures 2a, 2b, 5a, 5b, 7a, 7b, 7c, 7d, 7a<sup>+</sup>, and 7b<sup>+</sup> at the B3LYP level.<sup>41</sup> The basis set used for rhenium was effective-core-potential (ECP) based LANL2DZ basis,<sup>42</sup> with reoptimized functions of Couty and Hall<sup>43</sup> and a set of polarization f function.<sup>44</sup> The 6-31G\*\* basis sets<sup>45</sup> were used for all H, C, N, O, and Cl atoms. The 6-311G\* basis sets<sup>46</sup> was used for S atoms. Solvation energies were obtained by applying the SMD solvation model<sup>47</sup> with default radii and nonelectrostatic terms. For 2a, 2b, 5a, 5b, 7a, 7b, 7c, and 7d, the solvent was ethanol; for 7a<sup>+</sup> and 7b<sup>+</sup>, the solvent was acetonitrile. Previous publications<sup>20,48</sup> have shown that this protocol yielded data matching experimental results for related complexes. All of the geometry optimization and thermochemistry results were gained using the Gaussian09 (Rev. D01) package of programs.<sup>49</sup>

**Perchlorate Reduction Catalysis in Homogeneous Solution.** Stock solutions of  $[Re(O)(L)_2][OTf]$  (20 mM in  $CD_3CN$ ),  $Me_2S$  (0.5 M in  $CD_3CN$ ), and  $LiClO_4$  (2 M in  $D_2O$ ) were sequentially mixed in a 5 mm NMR tube to yield a 0.5 mL of solution containing 0.1 M of  $ClO_4^-$ , 0.4 M of  $Me_2S$ , and 4 mM of Re (TON = 100) with an ~95/5 (v/v) ratio of  $CD_3CN/D_2O$ . Conversion of  $Me_2S$  to  $Me_2SO$ , which is coupled to  $ClO_4^-$  reduction, was monitored by <sup>1</sup>H NMR. Alternatively, 0.1 M of  $ClO_4^-$ , 0.4 M of  $Et_2S$ , and 16 mM of Re (TON = 25) were used in order to effectively monitor the transformation of Re complexes during the reaction.

**Perchlorate Reduction Catalysis in Heterogeneous  $Re(L)_2$ -Pd/C Material.** A 50 mL pear-shaped flask was sequentially loaded with  $Re(O)(L_{O-N})_2Cl$  (containing 1.25 mg Re), 25 mg of Pd/C, a magnetic stir bar, and 50 mL of water (pH 3.0, prepared by addition of 1 mM HCl). The flask was sealed with a rubber stopper, sonicated for 2 min with occasional shaking, and then placed in a 25 °C water bath. The suspension was stirred at 1100 rpm under 1 atm  $H_2$  (supplied through two stainless steel needles as gas inlet and outlet to the fumehood atmosphere) for 4 h to allow an adequate immobilization of the  $Re(O)(L_{O-N})_2Cl$  precursor into Pd/C matrix.<sup>17a</sup>  $NaClO_4$  stock solution (0.2 M in  $H_2O$ ) was then introduced in the catalyst suspension to initiate the reaction. Aqueous samples were periodically collected from the  $H_2$  outlet and immediately filtered (0.45- $\mu$ m cellulose membrane) to quench the reaction.  $ClO_4^-$  concentration was measured by ion chromatography (Dionex ICS-3000, IonPac AS16 column, 1.0 mL  $min^{-1}$  flow rate, 65 mM KOH eluent, 30 °C column temperature).  $Cl^-$  concentration was measured with an IonPac AS19 column (1.0 mL  $min^{-1}$  flow rate, 10 mM KOH eluent, and 30 °C column temperature) on the same system.

## ■ ASSOCIATED CONTENT

### 📄 Supporting Information

The Supporting Information is available free of charge on the ACS Publications website at DOI: 10.1021/acs.inorgchem.5b02940. CCDC 1440558 (structure 2a), 1440571 (2b), 1440485 (3), 1440486 (5a), 1440487 (5b), 1440488 (6), 1440489 (7a), and 1440490 (the  $C_2$ -symmetric aqua complex) contain the supplementary crystallographic data for this paper. The data can be obtained free of charge from the Cambridge Crystallographic Data Centre at [www.ccdc.cam.ac.uk/getstructures](http://www.ccdc.cam.ac.uk/getstructures).

Experimental sections and additional materials as noted in the text (PDF)

Crystallographic data (CIF)

## AUTHOR INFORMATION

### Corresponding Authors

\*(J.L.) E-mail: [jyliu@mines.edu](mailto:jyliu@mines.edu); [jinyongliu101@gmail.com](mailto:jinyongliu101@gmail.com).

\*(T.J.S.) E-mail: [strthmnn@mines.edu](mailto:strthmnn@mines.edu).

### Present Addresses

D.W.: Room B-901, Hong Ta Xiao Qu, Anhai, Jinjiang, Fujian 362261, P.R. China.

S.K.: Department of Chemistry and Biochemistry, University of South Carolina, Columbia, South Carolina 29208, United States.

### Notes

The authors declare no competing financial interest.

## ACKNOWLEDGMENTS

Financial support was provided by the National Science Foundation (CBET-1555549) and the U.S. EPA Science to Achieve Results Program (Grant #RD83517401). Professor Kenneth Suslick, Professor Gregory Girolami (UIUC), and Dr. Zhenggang Xu (Texas A&M University) are acknowledged for helpful discussions. Dr. Dean Olson and Dr. Mike Hallock (UIUC) are, respectively, acknowledged for assistance with NMR measurements and DFT calculations. Dr. Jeffery Bertke, Dr. Amy Fuller, and Ms. Hyunjin Lee (UIUC) conducted the crystallography analysis.

## REFERENCES

- (1) (a) Kühn, F. E.; Scherbaum, A.; Herrmann, W. A. *J. Organomet. Chem.* **2004**, *689*, 4149–4164. (b) Owens, G. S.; Arias, J.; Abu-Omar, M. M. *Catal. Today* **2000**, *55*, 317–363. (c) Sousa, S. C.; Cabrita, I.; Fernandes, A. C. *Chem. Soc. Rev.* **2012**, *41*, 5641–5653. (d) Martins, L. M.; Alegria, E. C.; Smoleński, P.; Kuznetsov, M. L.; Pombeiro, A. J. *Inorg. Chem.* **2013**, *52*, 4534–4546. (e) Lilly, C. P.; Boyle, P. D.; Ison, E. A. *Organometallics* **2012**, *31*, 4295–4301. (f) Alegria, E. C.; Kirillova, M. V.; Martins, L. M.; Pombeiro, A. J. *Appl. Catal., A* **2007**, *317*, 43–52. (g) Kirillov, A. M.; Haukka, M.; Kirillova, M. V.; Pombeiro, A. J. *Adv. Synth. Catal.* **2005**, *347*, 1435–1446. (h) Lippert, C. A.; Arnstein, S. A.; Sherrill, C. D.; Soper, J. D. *J. Am. Chem. Soc.* **2010**, *132*, 3879–3892. (i) Dinda, S.; Genest, A.; Rösch, N. *ACS Catal.* **2015**, *5*, 4869–4880.
- (2) (a) Raju, S.; Moret, M.-E.; Klein Gebbink, R. J. *ACS Catal.* **2015**, *5*, 281–300. (b) Michael McClain, J.; Nicholas, K. M. *ACS Catal.* **2014**, *4*, 2109–2112. (c) Shiramizu, M.; Toste, F. D. *Angew. Chem., Int. Ed.* **2013**, *52*, 12905–12909. (d) Yi, J.; Liu, S.; Abu-Omar, M. M. *ChemSusChem* **2012**, *5*, 1401–1404.
- (3) (a) Jürgens, S.; Herrmann, W. A.; Kühn, F. E. *J. Organomet. Chem.* **2014**, *751*, 83–89. (b) Le Bideau, F.; Dagorne, S. *Chem. Rev.* **2013**, *113*, 7793–7850. (c) Abram, U.; Alberto, R. J. *Braz. Chem. Soc.* **2006**, *17*, 1486–1500. (d) Aufort, M.; Gonera, M.; Le Gal, J.; Czarny, B.; Le Clainche, L.; Thai, R.; Dugave, C. *ChemBioChem* **2011**, *12*, 583–592. (e) Nguyen, H. H.; Pham, C. T.; Abram, U. *Inorg. Chem.* **2015**, *54*, 5949–5959.
- (4) Sen, S.; Mukherjee, T.; Sarkar, S.; Mukhopadhyay, S. K.; Chattopadhyay, P. *Analyst* **2011**, *136*, 4839–4845.
- (5) (a) Shuter, E.; Hoveyda, H.; Karunaratne, V.; Rettig, S. J.; Orvig, C. *Inorg. Chem.* **1996**, *35*, 368–372. (b) Kühn, F. E.; Rauch, M. U.; Lobmaier, G. M.; Artus, G. R.; Herrmann, W. A. *Chem. Ber.* **1997**, *130*, 1427–1431. (c) Shan, X.; Ellern, A.; Espenson, J. H. *Inorg. Chem.* **2002**, *41*, 7136–7142. (d) Schröckeneder, A.; Traar, P.; Raber, G.; Baumgartner, J.; Belaj, F.; Mösch-Zanetti, N. C. *Inorg. Chem.* **2009**, *48*, 11608–11614. (e) Traar, P.; Schachner, J. A.; Steiner, L.; Sachse, A.; Volpe, M.; Mösch-Zanetti, N. C. *Inorg. Chem.* **2011**, *50*, 1983–1990. (f) Zwettler, N.; Schachner, J. A.; Belaj, F.; Mösch-Zanetti, N. C. *Inorg. Chem.* **2014**, *53*, 12832–12840. (g) Machura, B.; Wolff, M.; Tabak, D.; Schachner, J. A.; Mösch-Zanetti, N. C. *Eur. J. Inorg. Chem.* **2012**, *2012*, 3764–3773. (h) Machura, B.; Kusz, J. *Polyhedron* **2008**, *27*, 187–195. (i) Machura, B.; Wolff, M.; Benoist, E.; Schachner, J. A.; Mösch-Zanetti, N. C. *Dalton Trans.* **2013**, *42*, 8827–8837. (j) Machura, B.; Kruszynski, R. *Polyhedron* **2007**, *26*, 2957–2963.
- (6) (a) Herrmann, W. A.; Rauch, M. U.; Artus, G. R. *Inorg. Chem.* **1996**, *35*, 1988–1991. (b) van Bommel, K. J.; Verboom, W.; Kooijman, H.; Spek, A. L.; Reinhoudt, D. N. *Inorg. Chem.* **1998**, *37*, 4197–4203. (c) Benny, P. D.; Barnes, C. L.; Piekarski, P. M.; Lydon, J. D.; Jurisson, S. S. *Inorg. Chem.* **2003**, *42*, 6519–6527. (d) Benny, P. D.; Green, J. L.; Engelbrecht, H. P.; Barnes, C. L.; Jurisson, S. S. *Inorg. Chem.* **2005**, *44*, 2381–2390.
- (7) Bergeron, R. J. *Chem. Rev.* **1984**, *84*, 587–602.
- (8) Abu-Omar, M. M.; McPherson, L. D.; Arias, J.; Béreau, V. M. *Angew. Chem., Int. Ed.* **2000**, *39*, 4310–4313.
- (9) (a) Ison, E. A.; Trivedi, E. R.; Corbin, R. A.; Abu-Omar, M. M. *J. Am. Chem. Soc.* **2005**, *127*, 15374–15375. (b) Du, G.; Abu-Omar, M. M. *Organometallics* **2006**, *25*, 4920–4923.
- (10) Ison, E. A.; Corbin, R. A.; Abu-Omar, M. M. *J. Am. Chem. Soc.* **2005**, *127*, 11938–11939.
- (11) Wegenhart, B. L.; Abu-Omar, M. M. *Inorg. Chem.* **2010**, *49*, 4741–4743.
- (12) Lin, A.; Peng, H.; Abdukader, A.; Zhu, C. *Eur. J. Org. Chem.* **2013**, *2013*, 7286–7290.
- (13) (a) Greer, M. A.; Goodman, G.; Pleus, R. C.; Greer, S. E. *Environ. Health Perspect.* **2002**, *110*, 927–937. (b) Braverman, L. E.; He, X.; Pino, S.; Cross, M.; Magnani, B.; Lamm, S. H.; Kruse, M. B.; Engel, A.; Crump, K. S.; Gibbs, J. P. *J. Clin. Endocrinol. Metab.* **2005**, *90*, 700–706.
- (14) (a) Blount, B. C.; Alwis, K. U.; Jain, R. B.; Solomon, B. L.; Morrow, J. C.; Jackson, W. A. *Environ. Sci. Technol.* **2010**, *44*, 9564–9570. (b) Parker, D. R.; Seyffarth, A. L.; Reese, B. K. *Environ. Sci. Technol.* **2008**, *42*, 1465–1471.
- (15) (a) Wang, Z.; Forsyth, D.; Lau, B. P. Y.; Pelletier, L.; Bronson, R.; Gaertner, D. J. *Agric. Food Chem.* **2009**, *57*, 9250–9255. (b) Jackson, W. A.; Joseph, P.; Laxman, P.; Tan, K.; Smith, P. N.; Yu, L.; Anderson, T. A. *J. Agric. Food Chem.* **2005**, *53*, 369–373.
- (16) U.S. Environmental Protection Agency. *Fed. Regist.* **2011**, *76*, 7762–7767.
- (17) (a) Liu, J.; Choe, J. K.; Wang, Y.; Shapley, J. R.; Werth, C. J.; Strathmann, T. J. *ACS Catal.* **2015**, *5*, 511–522. (b) Zhang, Y.; Hurley, K. D.; Shapley, J. R. *Inorg. Chem.* **2011**, *50*, 1534–1543. (c) Liu, J.; Chen, X.; Wang, Y.; Strathmann, T. J.; Werth, C. J. *Environ. Sci. Technol.* **2015**, *49*, 12932–12940.
- (18) Holm, R. *Chem. Rev.* **1987**, *87*, 1401–1449.
- (19) (a) Liu, J.; Choe, J. K.; Sasnow, Z.; Werth, C. J.; Shapley, J. R.; Strathmann, T. J. In *INOR: Energy and Environmental Related Inorganic Chemistry*; Abstract #195 of the 244th ACS National Meeting, Philadelphia, PA, Aug 19–23, 2012; American Chemical Society: Washington, DC, 2012. (b) Liu, J.; Kimura, S. Y.; Choe, J. K.; Shapley, J. R.; Werth, C. J.; Strathmann, T. J. In *INOR: Energy and Environmental Related Inorganic Chemistry*; Abstract #712 of the 248th ACS National Meeting, San Francisco, CA, Aug 10–14, 2014; American Chemical Society: Washington, DC, 2014.
- (20) Schachner, J. A.; Terfassa, B.; Peschel, L. M.; Niklas, Z.; Belaj, F.; Cias, P.; Gescheidt, G.; Mösch-Zanetti, N. C. *Inorg. Chem.* **2014**, *53*, 12918–12928.
- (21) Machura, B.; Wolff, M.; Gryca, I. *Coord. Chem. Rev.* **2014**, *275*, 154–164.
- (22) Lobmaier, G. M.; Frey, G. D.; Dewhurst, R. D.; Herdtweck, E.; Herrmann, W. A. *Organometallics* **2007**, *26*, 6290–6299.
- (23) (a) Arias, J.; Newlands, C. R.; Abu-Omar, M. M. *Inorg. Chem.* **2001**, *40*, 2185–2192. (b) McPherson, L. D.; Drees, M.; Khan, S. I.; Strassner, T.; Abu-Omar, M. M. *Inorg. Chem.* **2004**, *43*, 4036–4050.
- (24) Cordone, R.; Taube, H. *J. Am. Chem. Soc.* **1987**, *109*, 8101–8102.
- (25) (a) Melanson, R.; Rochon, F. *Can. J. Chem.* **1976**, *54*, 1002–1006. (b) Rochon, F.; Kong, P.; Melanson, R. *Can. J. Chem.* **1980**, *58*, 97–101.

- (26) Brown, H. C.; Kanner, B. J. *Am. Chem. Soc.* **1953**, *75*, 3865–3865.
- (27) (a) Machura, B.; Wolff, M.; Benoist, E.; Schachner, J.; Möscher-Zanetti, N.; Takao, K.; Ikeda, Y. *Polyhedron* **2014**, *69*, 205–218. (b) Machura, B.; Kusz, J.; Tabak, D.; Kruszynski, R. *Polyhedron* **2009**, *28*, 493–500. (c) Machura, B.; Wolff, M.; Kruszynski, R.; Kusz, J. *Polyhedron* **2009**, *28*, 1211–1220. (d) Machura, B.; Wolff, M.; Kusz, J.; Kruszynski, R. *Polyhedron* **2009**, *28*, 2949–2964. (e) Machura, B.; Wolff, M.; Kowalczyk, W.; Musiol, R. *Polyhedron* **2012**, *33*, 388–395. (f) Machura, B.; Wolff, M. *Struct. Chem.* **2014**, *25*, 1607–1623.
- (28) Friebolin, H. *Basic One- and Two-Dimensional NMR Spectroscopy*, 5th ed.; Wiley-VCH: Weinheim, Germany, 2011; pp 313–342.
- (29) *Barstow Groundwater Perchlorate Contamination*; California Regional Water Quality Control Board, Lahontan Region: South Lake Tahoe, CA, 2012.
- (30) Choe, J. K.; Mehnert, M. H.; Guest, J. S.; Strathmann, T. J.; Werth, C. J. *Environ. Sci. Technol.* **2013**, *47*, 4644–4652.
- (31) (a) Hurley, K. D.; Shapley, J. R. *Environ. Sci. Technol.* **2007**, *41*, 2044–2049. (b) Choe, J. K.; Shapley, J. R.; Strathmann, T. J.; Werth, C. J. *Environ. Sci. Technol.* **2010**, *44*, 4716–4721. (c) Liu, J.; Choe, J. K.; Sasnow, Z. D.; Werth, C. J.; Strathmann, T. J. *Water Res.* **2013**, *47*, 91–101. (d) Choe, J. K.; Boyanov, M. I.; Liu, J.; Kemner, K. M.; Werth, C. J.; Strathmann, T. J. *J. Phys. Chem. C* **2014**, *118*, 11666–11676.
- (32) (a) Judmaier, M. E.; Holzer, C.; Volpe, M.; Möscher-Zanetti, N. C. *Inorg. Chem.* **2012**, *51*, 9956–9966. (b) Schachner, J. A.; Traar, P.; Sala, C.; Melcher, M.; Harum, B. N.; Sax, A. F.; Volpe, M.; Belaj, F.; Möscher-Zanetti, N. C. *Inorg. Chem.* **2012**, *51*, 7642–7649. (c) Brito, J. A.; Ladeira, S.; Teuma, E.; Royo, B.; Gómez, M. *Appl. Catal., A* **2011**, *398*, 88–95. (d) Brito, J. A.; Gómez, M.; Muller, G.; Teruel, H.; Clinet, J. C.; Duñach, E.; Maestro, M. A. *Eur. J. Inorg. Chem.* **2004**, *2004*, 4278–4285. (e) Nunes, C. D.; Valente, A. A.; Pillinger, M.; Fernandes, A. C.; Romão, C. C.; Rocha, J.; Gonçalves, I. S. *J. Mater. Chem.* **2002**, *12*, 1735–1742.
- (33) (a) Peschel, L. M.; Belaj, F.; Möscher-Zanetti, N. C. *Angew. Chem., Int. Ed.* **2015**, *54*, 13018–13021. (b) Lehtonen, A.; Sillanpää, R. *Inorg. Chem.* **2004**, *43*, 6501–6506. (c) Levason, W.; McAuliffe, C.; McCullough, F., Jr. *Inorg. Chem.* **1977**, *16*, 2911–2916.
- (34) Hoveyda, H.; Karunaratne, V.; Rettig, S. J.; Orvig, C. *Inorg. Chem.* **1992**, *31*, 5408–5416.
- (35) APEX2; Bruker AXS, Inc.: Madison, WI, 2004.
- (36) SAINT, SHELXTL, XCIF, XPREP; Bruker AXS, Inc.: Madison, WI, 2005.
- (37) SADABS; Bruker AXS, Inc.: Madison, WI, 2007.
- (38) Sheldrick, G. M. *SHELXS-97, 97-2*; University of Göttingen: Göttingen, Germany, 1997.
- (39) Sheldrick, G. M. *SHELXL-97, 97-2*; University of Göttingen: Göttingen, Germany, 1997.
- (40) (a) Hohenberg, P.; Kohn, W. *Phys. Rev.* **1964**, *136*, B864–B871. (b) Kohn, W.; Sham, L. J. *Phys. Rev.* **1965**, *140*, A1133–A1138.
- (41) (a) Becke, A. D. *J. Chem. Phys.* **1993**, *98*, 5648–5652. (b) Lee, C.; Yang, W.; Parr, R. G. *Phys. Rev. B: Condens. Matter Mater. Phys.* **1988**, *37*, 785–789. (c) Devlin, F.; Finley, J.; Stephens, P.; Frisch, M. J. *Phys. Chem.* **1995**, *99*, 16883–16902.
- (42) Wadt, W. R.; Hay, P. J. *J. Chem. Phys.* **1985**, *82*, 284–298.
- (43) Couty, M.; Hall, M. B. *J. Comput. Chem.* **1996**, *17*, 1359–1370.
- (44) Ehlers, A.; Böhme, M.; Dapprich, S.; Gobbi, A.; Höllwarth, A.; Jonas, V.; Köhler, K.; Stegmann, R.; Veldkamp, A.; Frenking, G. *Chem. Phys. Lett.* **1993**, *208*, 111–114.
- (45) (a) Hehre, W. J.; Ditchfield, R.; Pople, J. A. *J. Chem. Phys.* **1972**, *56*, 2257–2261. (b) Hariharan, P. C.; Pople, J. A. *Theor. Chim. Acta* **1973**, *28*, 213–222.
- (46) (a) McLean, A.; Chandler, G. J. *J. Chem. Phys.* **1980**, *72*, 5639–5648. (b) Krishnan, R.; Binkley, J. S.; Seeger, R.; Pople, J. A. *J. Chem. Phys.* **1980**, *72*, 650–654.
- (47) Marenich, A. V.; Cramer, C. J.; Truhlar, D. G. *J. Phys. Chem. B* **2009**, *113*, 6378–6396.
- (48) Travia, N. E.; Xu, Z.; Keith, J. M.; Ison, E. A.; Fanwick, P. E.; Hall, M. B.; Abu-Omar, M. M. *Inorg. Chem.* **2011**, *50*, 10505–10514.
- (49) Frisch, M. J.; Trucks, G. W.; Schlegel, H. B.; Scuseria, G. E.; Robb, M. A.; Cheeseman, J. R.; Scalmani, G.; Barone, V.; Mennucci, B.; Petersson, G. A.; Nakatsuji, H.; Caricato, M.; Li, X.; Hratchian, H. P.; Izmaylov, A. F.; Bloino, J.; Zheng, G.; Sonnenberg, J. L.; Hada, M.; Ehara, M.; Toyota, K.; Fukuda, R.; Hasegawa, J.; Ishida, M.; Nakajima, T.; Honda, Y.; Kitao, O.; Nakai, H.; Vreven, T.; Montgomery, J. A., Jr.; Peralta, J. E.; Ogliaro, F.; Bearpark, M.; Heyd, J. J.; Brothers, E.; Kudin, K. N.; Staroverov, V. N.; Kobayashi, R.; Normand, J.; Raghavachari, K.; Rendell, A.; Burant, J. C.; Iyengar, S. S.; Tomasi, J.; Cossi, M.; Rega, N.; Millam, N. J.; Klene, M.; Knox, J. E.; Cross, J. B.; Bakken, V.; Adamo, C.; Jaramillo, J.; Gomperts, R.; Stratmann, R. E.; Yazyev, O.; Austin, A. J.; Cammi, R.; Pomelli, C.; Ochterski, J. W.; Martin, R. L.; Morokuma, K.; Zakrzewski, V. G.; Voth, G. A.; Salvador, P.; Dannenberg, J. J.; Dapprich, S.; Daniels, A. D.; Farkas, Ö.; Foresman, J. B.; Ortiz, J. V.; Cioslowski, J.; Fox, D. J. *Gaussian 09*; Gaussian, Inc.: Wallingford, CT, 2009.